Day 2.
Chemical evolution of the Milky Way

Chiaki Kobayashi
(Univ. of Hertfordshire, UK)

Contents

Day2: Galactic Chemical Evolution (GCE)

- Introduction
- Initial Mass Function (IMF)
- Basic equations of One-zone models
- Type Ia Supernova (SNIa) Model in GCE
- The Solar Neighborhood
- The Milky Way Galaxy
- Chemodynamical Simulations of a Milky Way-type galaxy
- Abundance Fitting, PopIII Nucleosynthesis, and Faint Supernova

Day3: Cosmic chemical evolution

- Basic equations of Chemodynamical Simulations

Chemical Evolution

Nomoto, Tominaga, CK 2013, ARAA

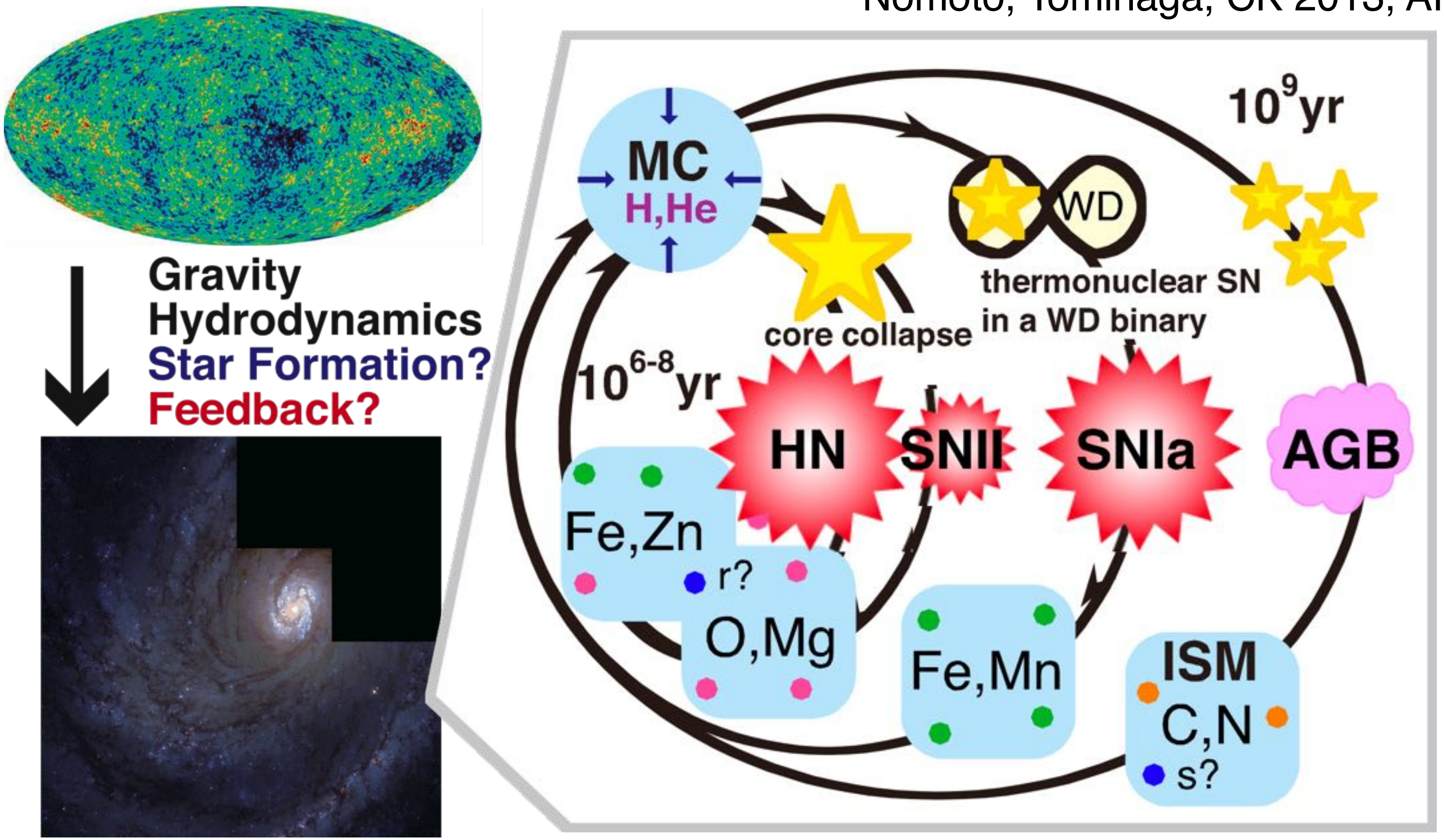

- [Fe/H] and [X/Fe] evolve in a galaxy: fossils that retain the evolution history of the galaxy → **Galactic Archaeology**

3 types of galaxy models

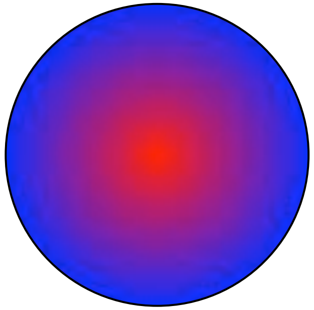

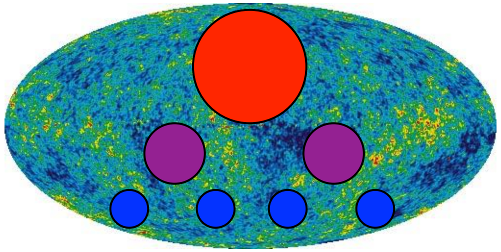

One-zone (monolithic) models (Tinsley 80, Timmes+ 95, Pagel 97, Matteucci 01, Prantzos + 93, Chiappini+ 97, CK+ 00 …)

Semi-analytic (hierarchical) models (Kauffmann, White + 93, Cole+ 94, Somerville & Primack 99, De Lucia+ 04, Nagashima+ 05 …)

Chemo-dynamical simulations (Burkert & Hensler 87, Katz 92, Navarro & White 93, Steinmetz & Müller 94, Mihos & Hernquist 94, … Kawata & Gibson 03, CK 04, … CK & Nakasato 11, Scannapieco+ 11, GASOLINE, RAMSES**,** AREPO…)

Other types of models

- Stochastic models (Argast+02; Ishimaru & Prantzos; Cescutti+; Wehmeyer+)
- Chemodynamical models without hydro (e.g., Minchev & Chiappini)

3 types of galaxy models

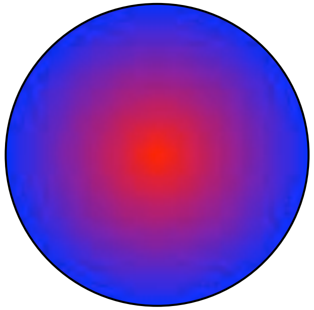

One-zone (monolithic) models

- Instantaneous mixing approximation
- SFR/inflow/outflow with analytic formula
- Average evolution of a galaxy (or a shell of galaxy)

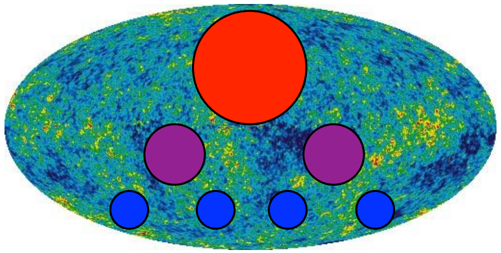

Semi-analytic (hierarchical) models

- Mass assembly history based on λCDM scenario
- Global properties of galaxies in a large scale

Chemo-dynamical simulations

- Inhomogeneous chemical enrichment
- Internal structures - kinematics of stars/gas, spatial distribution of elements

Other types of models

- Stochastic models (Argast+02; Ishimaru & Prantzos; Cescutti+; Wehmeyer+)
- Chemodynamical models without hydro (e.g., Minchev & Chiappini)

[α/Fe]-[Fe/H] relation

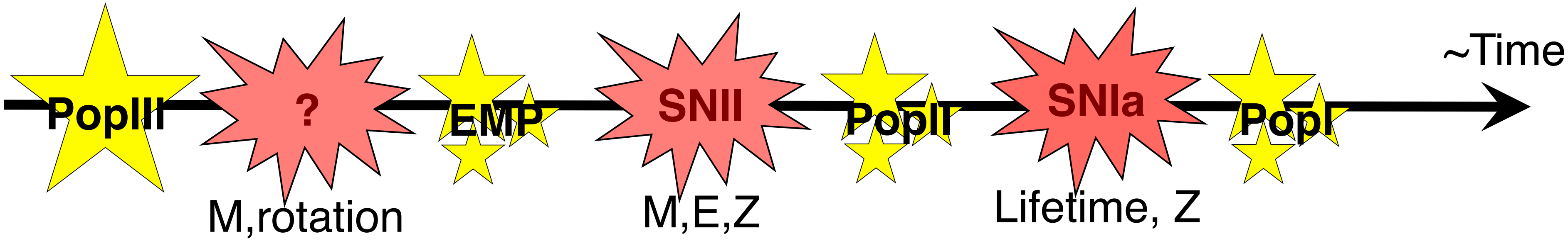

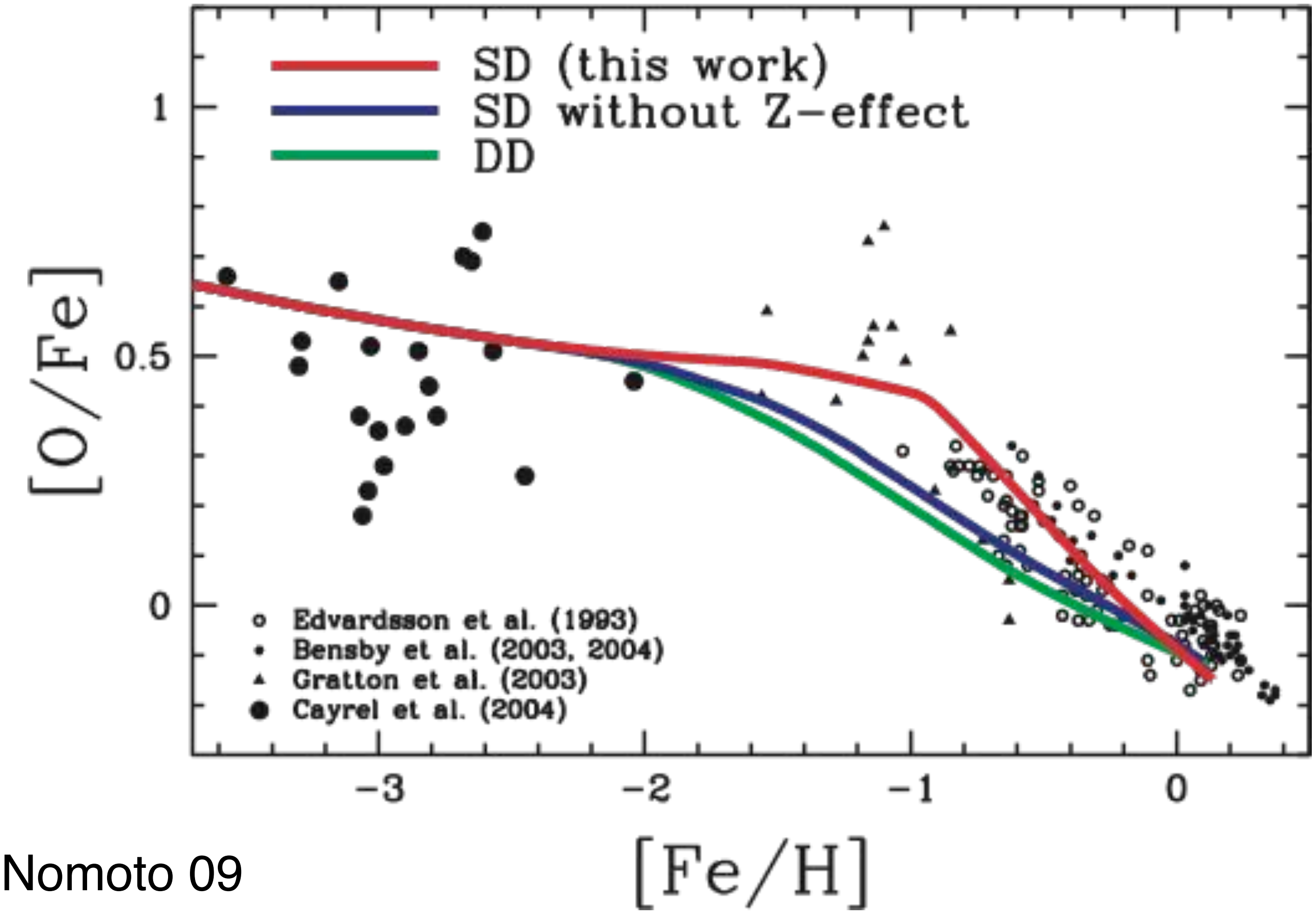

CK+98; CK & Nomoto 09

NLTE abundances

Zhao, Mashonkina, CK et al. 2016

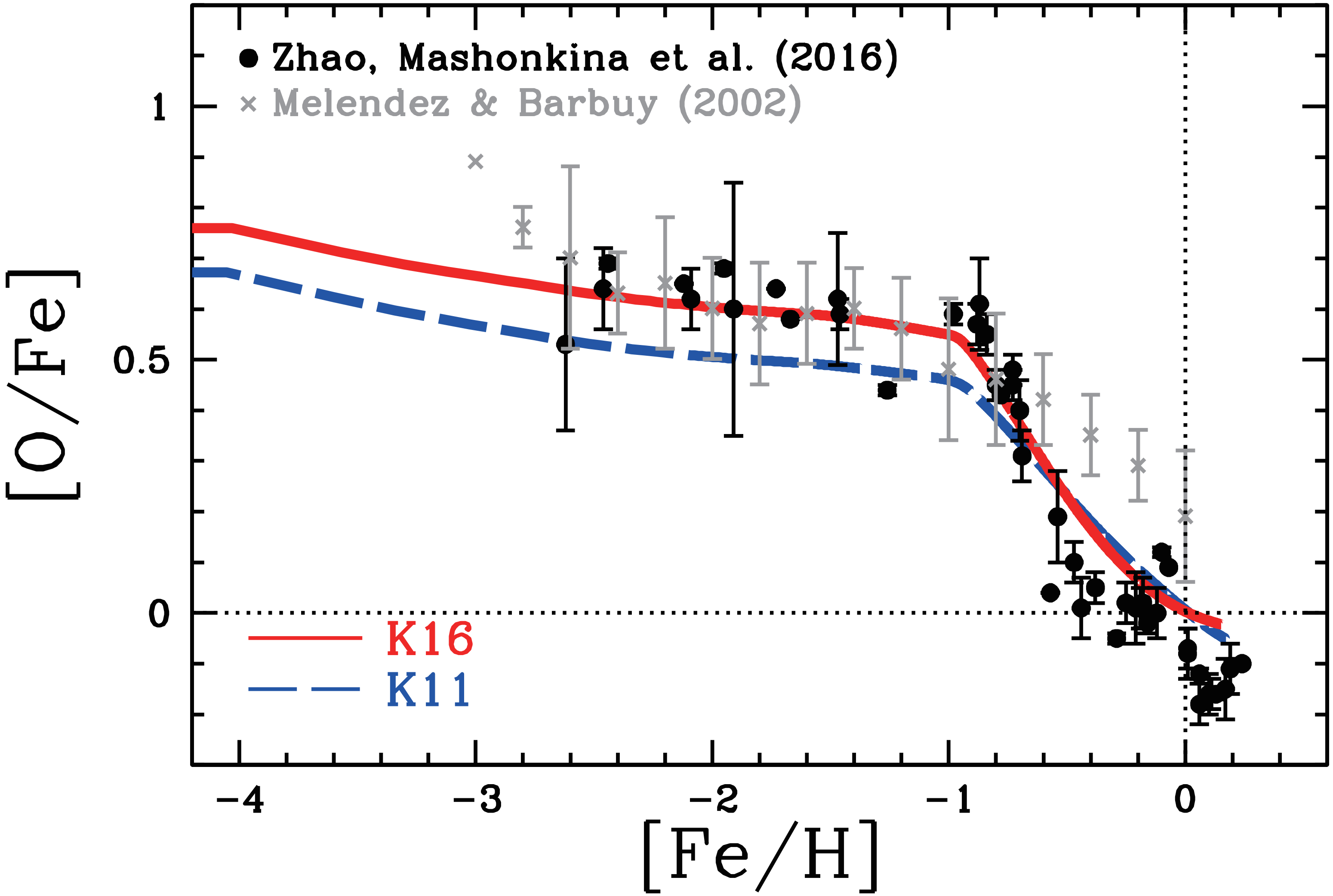

- 51 stars, 48 from Shane/Hamilton R~60000

Solar abundance (Asplund+09)

New atomic data

Sneden, Cowan, CK, et al 2015

✷ HD 84937, [Fe/H]=-2.32

✷ LTE analysis OK

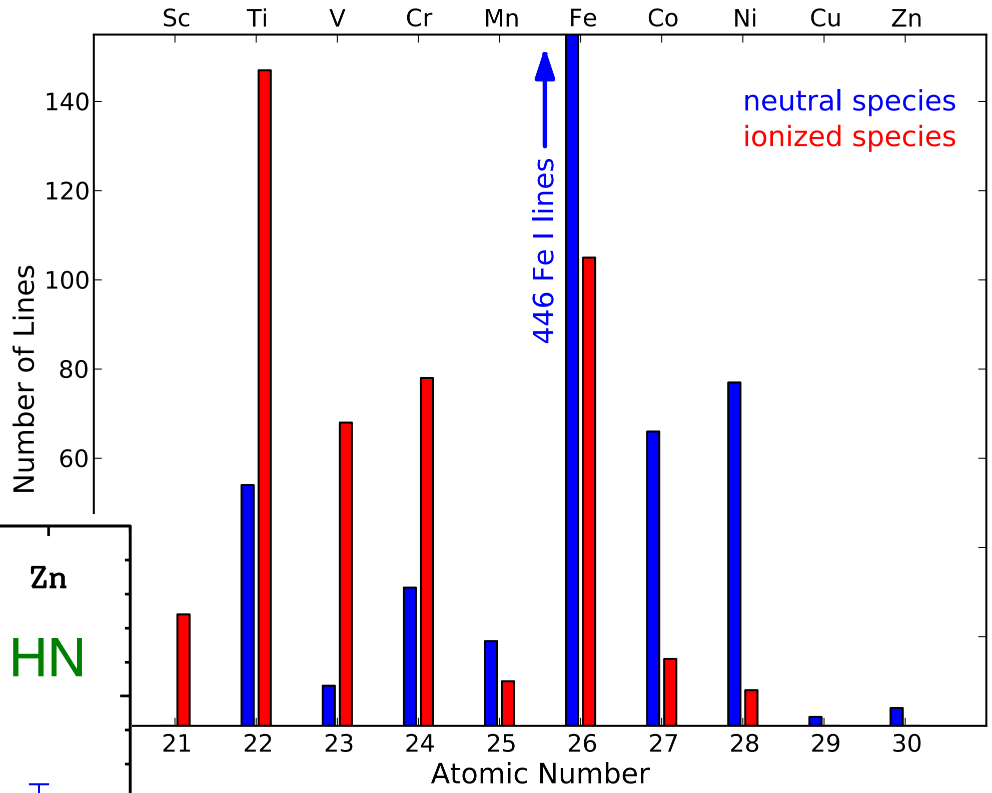

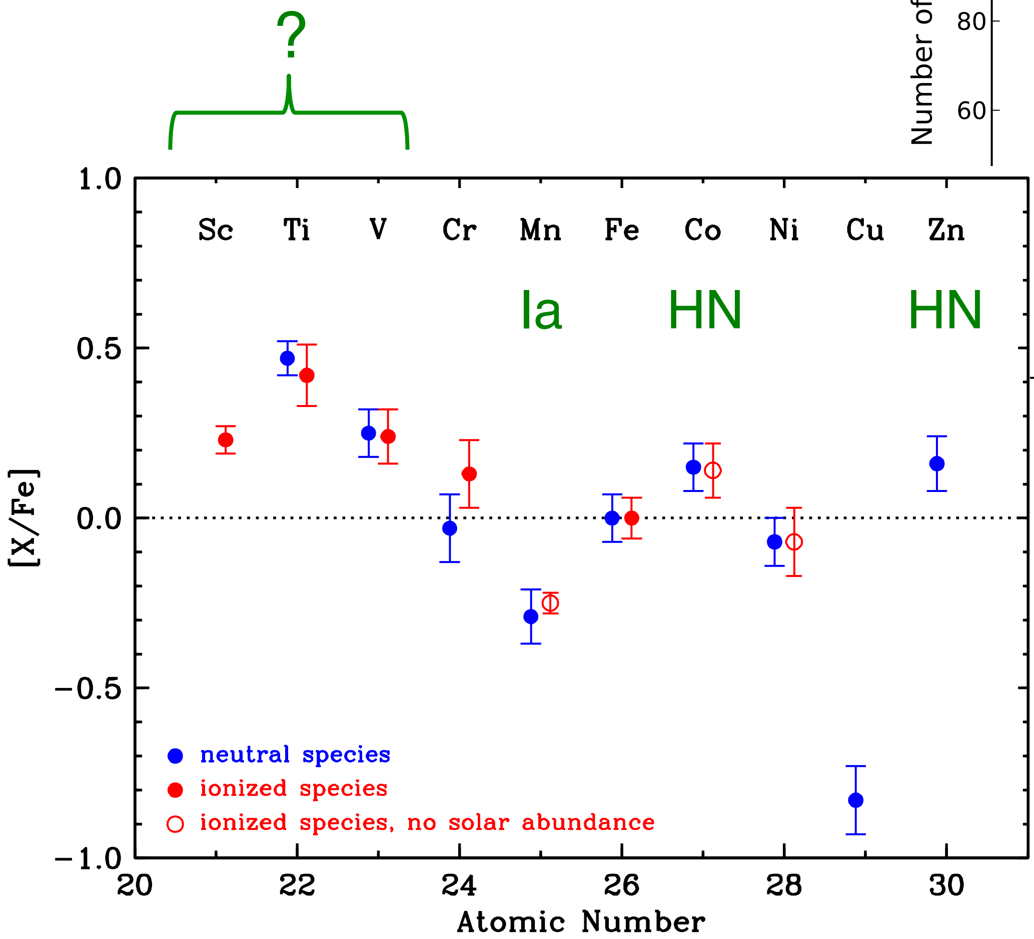

Stellar Yields

Nomoto, Kobayashi, Tominaga 2013, ARAA (1D, no rotation)

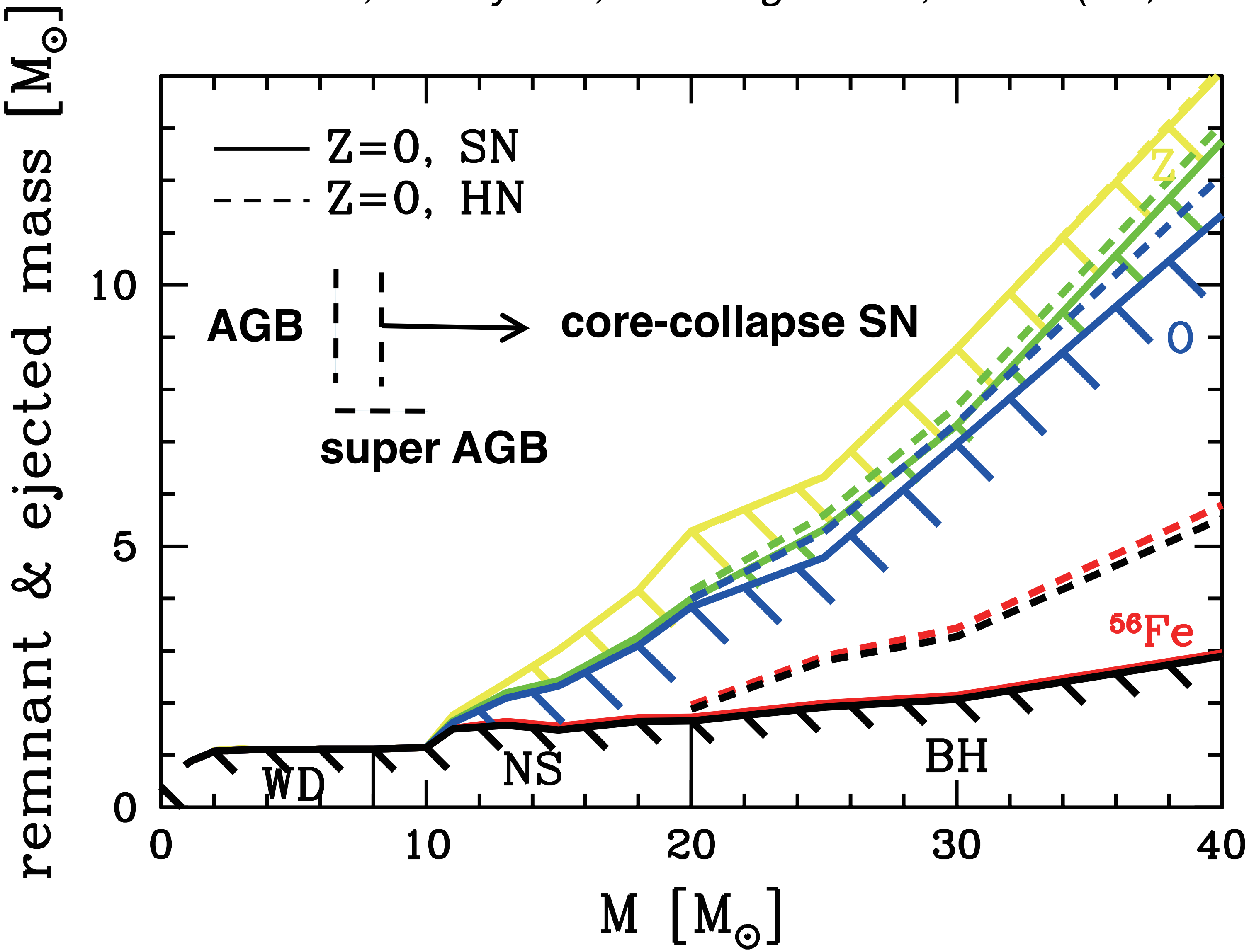

Also, Woosley & Heger; Limongi & Chieffi

Initial Mass Function (IMF)

Initial Mass Function (IMF)

- $\phi(m)$: the mass of stars formed in the mass interval (m, $m+dm$). Approximated by a power low, time-independent.

$$\phi(m) \propto m^{-x}$$

- normalized between the lower limit $m_\ell \sim 0.1\mathrm{M}_\odot$ and upper limit $m_\mathrm{u} \sim 120\mathrm{M}_\odot$

$$\int_{m_\ell}^{m_u} m^{-x} dm = \frac{1}{1-x}(m_u^{1-x} - m_\ell^{1-x}) = 1$$

$$\phi(m) = m^{-x} \frac{1-x}{m_u^{1-x} - m_\ell^{1-x}}$$

- Observed IMF has x=1.35 (Salpeter 1955), but universal?

※ If the IMF is defined for the number, x=2.35.

Initial Mass Function (IMF)

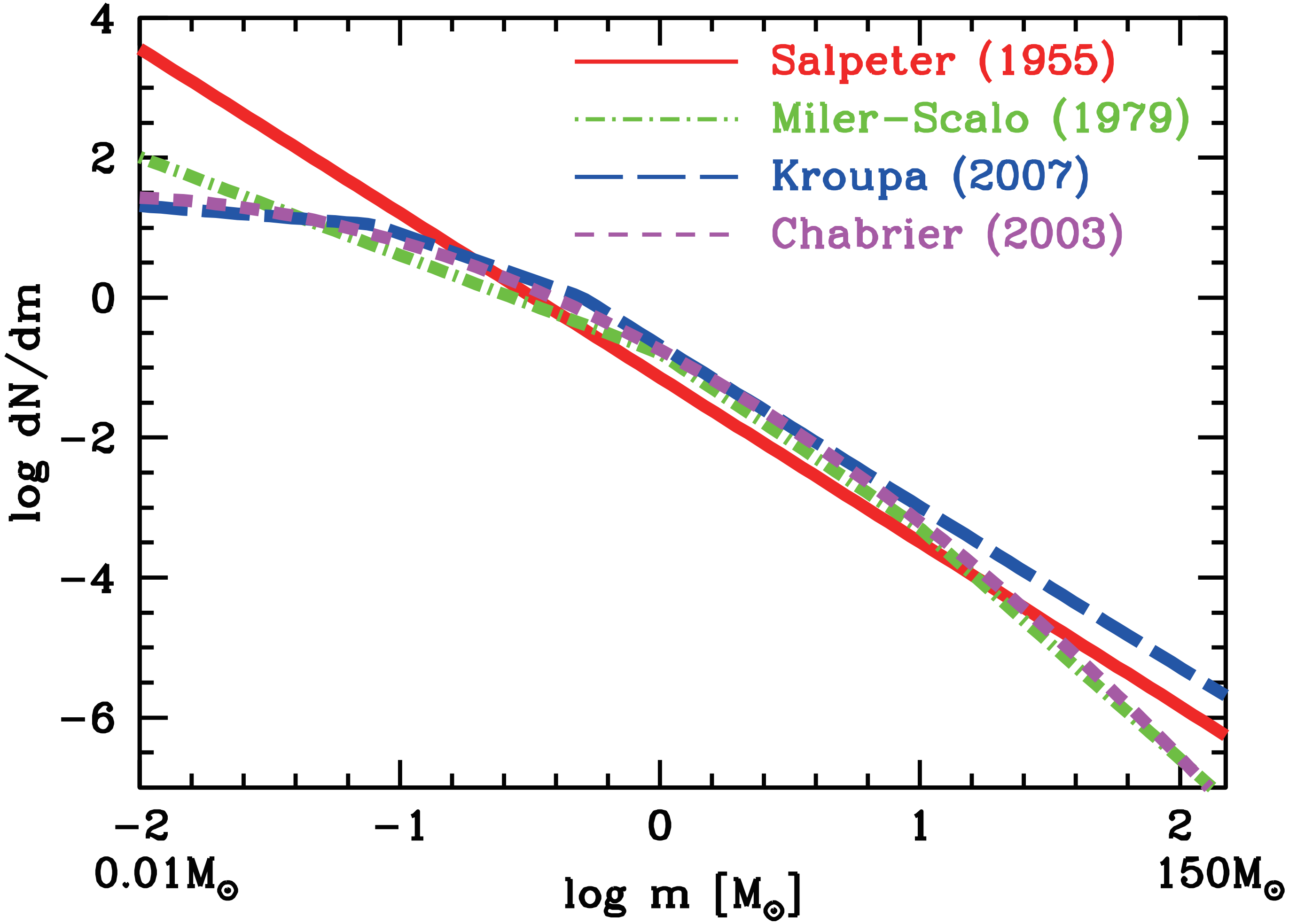

In GCE, Salpeter IMF with m_ℓ=0.07M$_\odot$ ~ Kroupa IMF

Universal IMF!

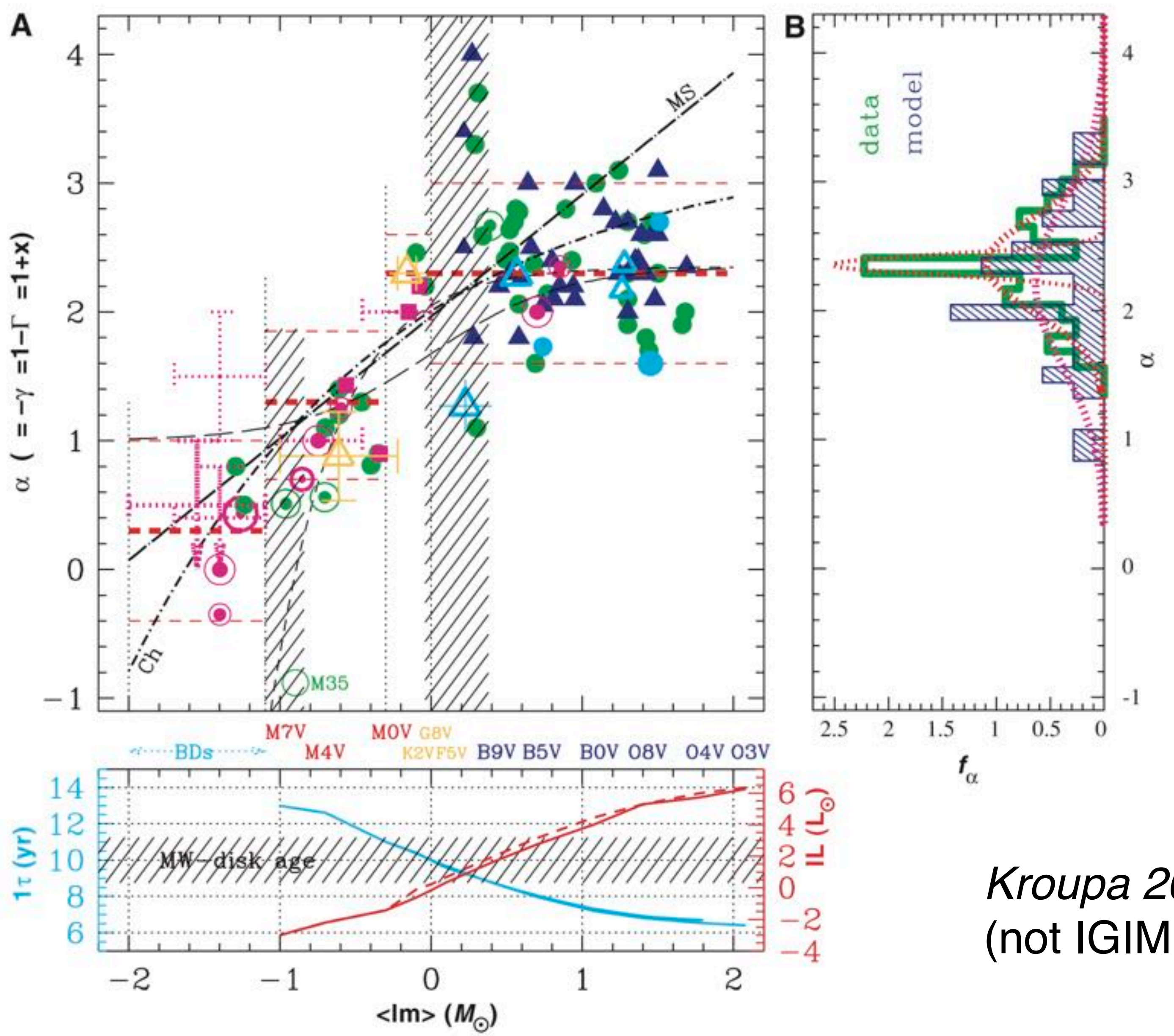

Kroupa 2002
(not IGIMF)

IMF is universal?

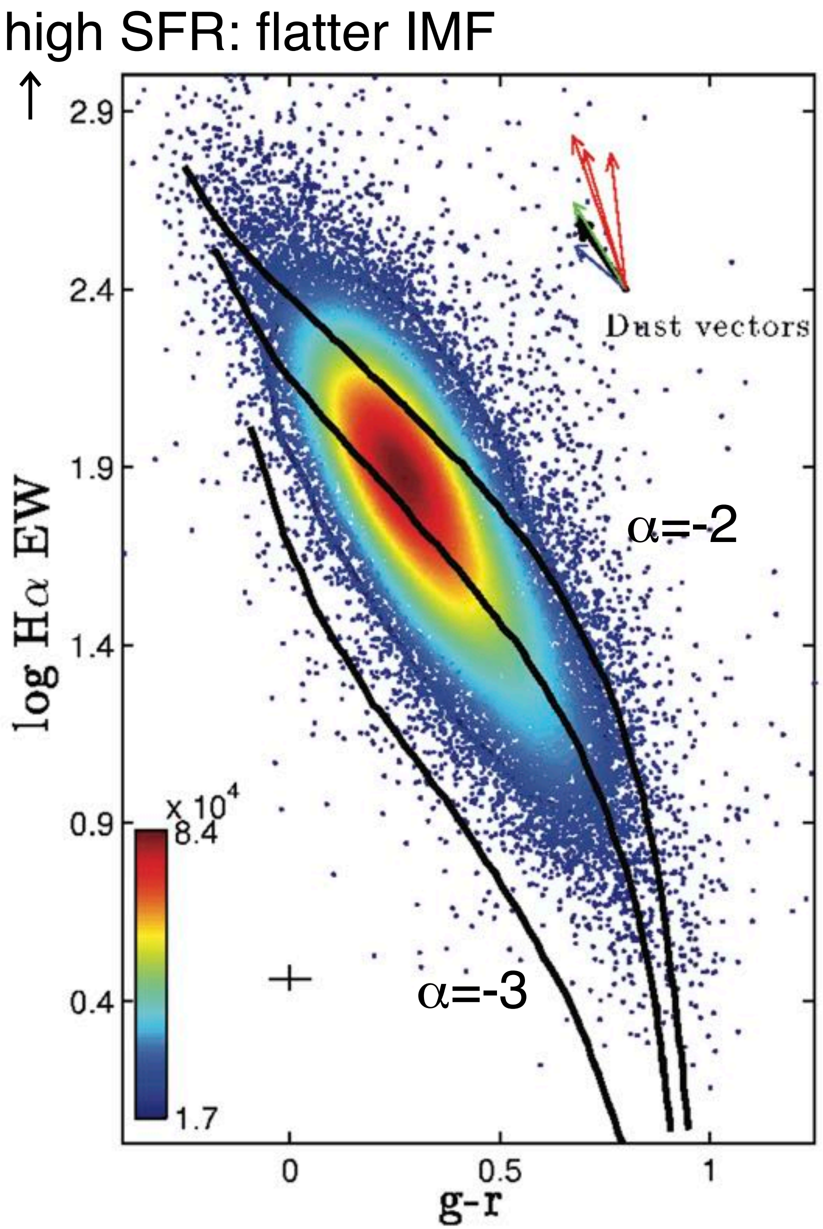

Figure 4. Distribution of all GAMA galaxies up to $z = 0.355$, after dust corrections as given in the text. All data and the model tracks are k-corrected to $z = 0.1$. The colour contours indicate the data density and the three solid lines indicate the three different evolutionary paths a galaxy would take if all star clusters within that galaxy have an IMF with a slope of $\alpha = -3$ (bottom track), $\alpha = -2.35$ (middle track) or $\alpha = -2$ (top track). These model tracks are generated using PÉGASE. The arrows depict the dust vectors. The red arrows represent radiative transfer model predictions calculated using the model of Popescu et al. (2000, 2011) and Tuffs et al. (2004) and from left to right correspond to $\tau_b = 8, 4, 1$, all assuming a median galaxy inclination of 60° and $F = 0.35$. The rest of the vectors show the movement of data points for different dust extinction curves and for a BD of 4. Blue: the dust vector calculated using the Calzetti (1997) curve for the continuum corrections and Cardelli et al. (1989) curve for emission-line corrections. Green: the dust vector corresponding to corrections calculated using Fischera & Dopita (2005) curve as modified by Wijesinghe et al. (2011). Black: the dust vector corresponding to the Calzetti (2001) and Cardelli et al. (1989) curves for the continuum and emission corrections, respectively.

GAMA (Galaxy and Mass Assembly)
120,000 galaxies
Gunawardhana, Hopkins, et al. 2011

IMF is universal?

→ massive, bottom heavy

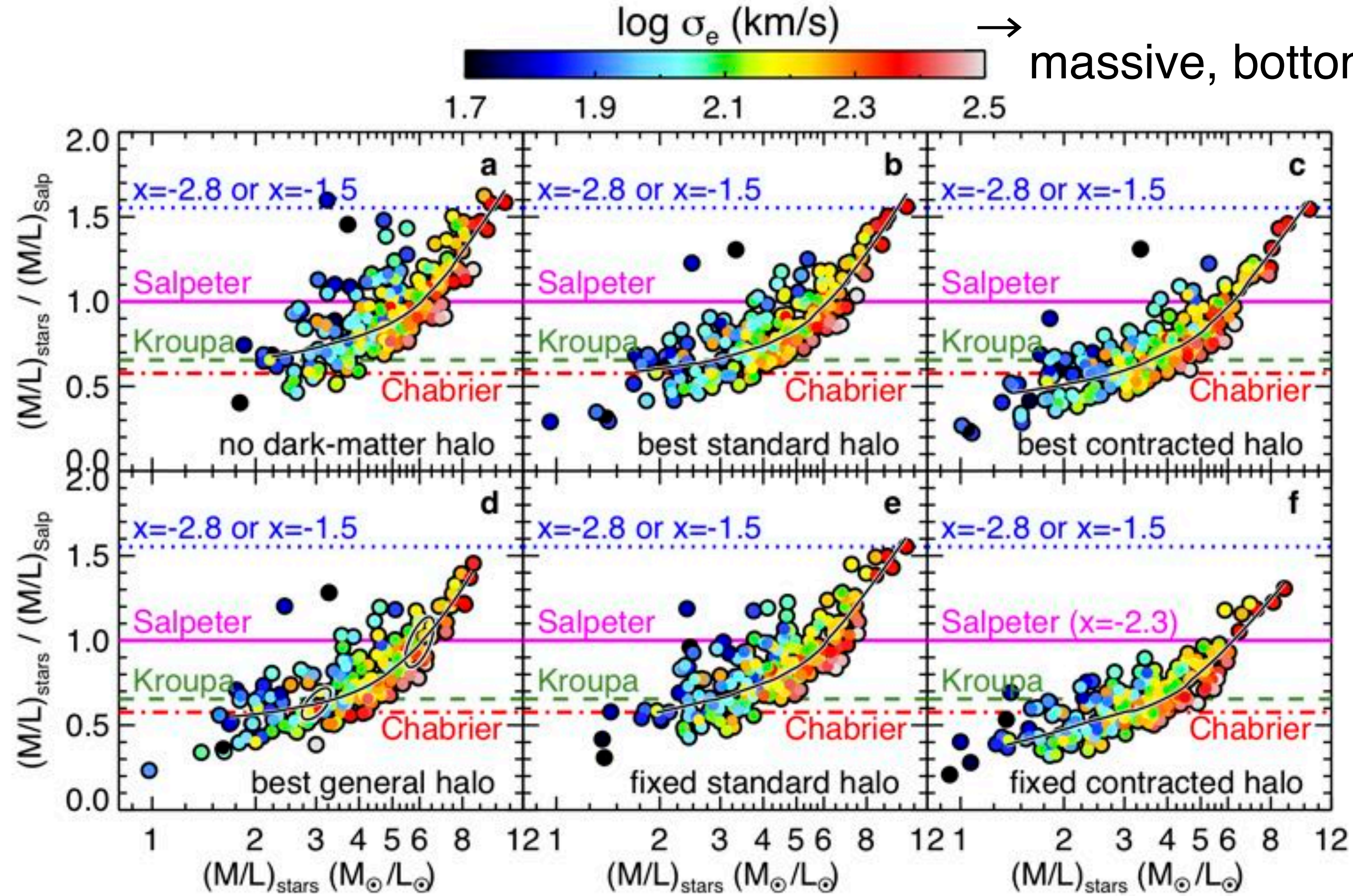

Figure 2 | The systematic variation of the IMF in early-type galaxies. The six panels show the ratio between the $(M/L)_{\rm stars}$ of the stellar component, determined using dynamical models, and the $(M/L)_{\rm Salp}$ of the stellar population, measured via stellar population models with a Salpeter IMF, as a function of $(M/L)_{\rm stars}$. The black solid line is a *loess* smoothed version of the data. Colours indicate the galaxies' stellar velocity dispersion $\sigma_{\rm e}$, which is related to the galaxy mass. The horizontal lines indicate the expected values for the ratio if the galaxy had (i) a Chabrier IMF (red dash-dotted line); (ii) a Kroupa IMF (green dashed line); (iii) a Salpeter IMF ($x = -2.3$, solid magenta line) and two additional power-law IMFs with (iv) $x = -2.8$ and (v) $x = -1.5$ respectively (blue dotted line). Different panels correspond to different assumptions for the dark matter halos employed in the dynamical models as written in the black titles. Details about the six sets of models are given in Table 1. A clear curved relation is visible in all panels. Panels **a**, **b** and **e** look quite similar, as for all of them the dark matter contributes only a small fraction (zero in **a** and a median of 12% in **b** and **e**) of the total mass inside a sphere with the projected size of the region where we have kinematics (about one projected half-light radius $R_{\rm e}$). Panel **f** with a fixed contracted halo, still shows the same IMF variation, but it is almost systematically lower by 35% in $(M/L)_{\rm stars}$ reflecting the increase in dark matter fraction. The two black thick ellipses plotted on top of the smooth relation in panel **d** show the representative 1σ error for one measurement at the given locations. We excluded from the plot the galaxies with very young stellar population (selected as having H$\beta > 2.3$ Å absorption). These galaxies have strong radial gradients in their population, which break our assumption of spatially constant M/L and makes both $(M/L)_{\rm Salp}$ and $(M/L)_{\rm stars}$ inaccurate.

ATLAS^{3D}
260 E-gals
Cappellari et al. 2012, Nature

IMF dependence of [α/Fe]

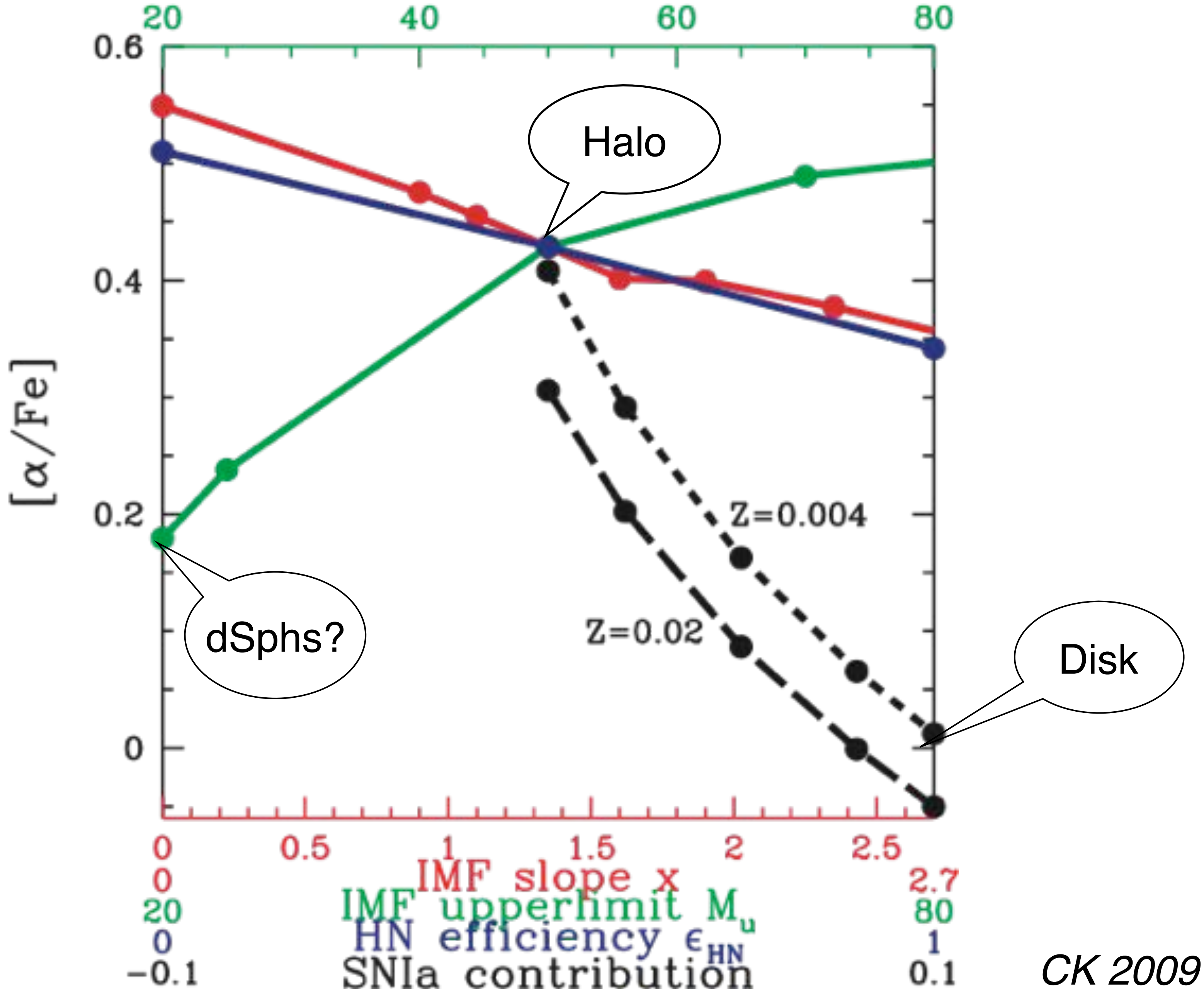

CK 2009

Basic equations of One-zone models

Tinsley 1980, Fundamentals of Cosmic Physics, 5, 287

Pagel 1997, Nucleosynthesis and Chemical Evolution of Galaxies

Matteucci 2001, The Chemical Evolution of the Galaxy

CK, Tsujimoto, Nomoto 2000, ApJ, 539, 26

One-zone model: basic equations

- Assumption: the interstellar medium (ISM) in a galaxy is well mixed, have uniform composition.
- Gas fraction f_g, star formation rate ψ, ejection rate E, E_{Ia}, infall rate R_{in}, outflow rate R_{out}

$$\frac{d\,f_{\rm g}}{dt} = -\psi + E + E_{\rm Ia} + R_{\rm in} - R_{\rm out}$$

- Stellar fraction f_s

$$\frac{d\,f_{\rm s}}{dt} = \psi - E - E_{\rm Ia}$$

- Metallicity Z: mass fraction of heavier elements than He

$$\frac{d\,(Z\,f_{\rm g})}{dt} = -Z\,\psi + E_Z + E_{Z,{\rm Ia}} + Z_{\rm in}\,R_{\rm in} - Z\,R_{\rm out}$$

Ejection rates from SWs and SNe

- Consider a star with initial mass m, lifetime τ_m, remnant mass fraction w_m. This star was born at time (t-τ_m) and dies at t.
- The mass with τ_m=t is called turnoff mass m_t.

$$E = \int_{m_t}^{m_u} (1 - w_m)\, \psi(t - \tau_m)\, \phi(m)\, dm \tag{1}$$

- Metals newly synthesized during AGB and core-collapse SNe; Nucleosynthesis yields p_{zm} depend on mass and metallicity of the star

$$E_{Z,\mathrm{cc}} = \int_{m_t}^{m_u} p_{zm}\, \psi(t - \tau_m)\, \phi(m)\, dm \tag{2}$$

- Metals that were in the star from its birth and re-ejected by stellar winds (SWs).

$$E_{Z,\mathrm{sw}} = \int_{m_t}^{m_u} (1 - w_m - p_{zm})\, Z(t - \tau_m)\, \psi(t - \tau_m)\, \phi(m)\, dm \tag{3}$$

One-zone model: analytic solution

$$E = \int_{m_t}^{m_u} (1 - w_m)\, \psi(t - \tau_m)\, \phi(m)\, dm \qquad (1)$$

- Instantaneous recycling approximation
  - ★ m_1 is the present turnoff mass
  - ★ $m>m_1$: immediately explode SNe
  - ★ $m<m_1$: never die
  - ★ neglect SNe Ia

$$E(t) = \int_{m_1}^{\infty} (1 - w_m)\psi(t)\phi(m)dm$$

$$R \equiv \int_{m_1}^{\infty} (1 - w_m)\phi(m)dm$$

$$E(t) = R\psi(t) \qquad (4)$$

- Returned fraction *R* is the fraction of mass put into stars at a given time that is thereafter returned to the ISM. ~0.4-0.5

One-zone model: analytic solution

$$E_{Z,\mathrm{sw}} = \int_{m_t}^{m_u} (1 - w_m - p_{zm})\, Z(t-\tau_m)\, \psi(t-\tau_m)\, \phi(m)\; dm \quad (2)$$

$$E_{Z,\mathrm{cc}} = \int_{m_t}^{m_u} p_{zm}\, \psi(t-\tau_m)\, \phi(m)\; dm \quad (3)$$

$$E_Z(t) = \int_{m_1}^{\infty} (1 - w_m - p_{zm}) Z(t) \psi(t) \phi(m) dm + \int_{m_1}^{\infty} p_{zm} \psi(t) \phi(m) dm$$

$$y \equiv \frac{1}{1-R} \int_{m_1}^{\infty} p_{zm} \psi(t) \phi(m) dm$$

$$E_Z(t) = RZ(t)\psi(t) + y(1-R)\big(1 - Z(t)\big)\psi(t)$$

- Net yield y is the mass of new metals ejected (eventually) when unit mass of matter is locked into stars. ~0.01-0.02
- If Z<<1

$$E_Z(t) = RZ(t)\psi(t) + y(1-R)\psi(t) \quad (5)$$

One-zone model: analytic solution

$$E(t) = R\psi(t) \tag{4}$$

$$E_Z(t) = RZ(t)\psi(t) + y(1-R)\psi(t) \tag{5}$$

- Basic equations are

$$\frac{df_s}{dt} = (1-R)\psi \tag{6}$$

$$\frac{df_g}{dt} = -(1-R)\psi + R_{\mathrm{in}} - R_{\mathrm{out}} \tag{7}$$

$$\frac{d(Zf_g)}{dt} = -Z(1-R)\psi + y(1-R)(1-Z)\psi + Z_{\mathrm{in}}R_{\mathrm{in}} - ZR_{\mathrm{out}} \tag{8}$$

- Metallicity evolution is

$$\frac{dZ}{dt} = \frac{1}{f_g}\left[\frac{d(Zf_g)}{dt} - Z\frac{df_g}{dt}\right] = \frac{1}{f_g}\left[y(1-R)(1-Z)\psi + (Z_{\mathrm{in}} - Z)R_{\mathrm{in}}\right]$$

Closed-box Model (i.e. Simple Model)

- A closed system, initially unenriched gas
- $R_{in}=R_{out}=0$, $f_g+f_s=1$
- Initial conditions $f_g(0)=1$, $f_s(0)=0$, $Z(0)=0$

$$\frac{dZ}{df_g}=\frac{1}{f_g}\frac{y(1-R)(1-Z)\psi}{-(1-R)\varphi}=\frac{-y(1-Z)}{f_g}$$

- if $Z<<1$

$$\frac{dZ}{df_g}=\frac{1}{f_g}\frac{y(1-R)\psi}{-(1-R)\varphi}=-y\frac{1}{f_g}$$

$$Z=\log f_g^{-y}=y\log f_g^{-1}$$

- if not

$$\frac{d(Z-1)}{df_g}=\frac{y(Z-1)}{f_g}$$

$$Z=1-f_g^{y} \quad \rightarrow 1 \quad \text{as} \quad f_g\rightarrow 0$$

Infall Model

- A system with infall balanced by star formation
- $R_{in} = (1\text{-}R)\psi$, R_{out}=0, f_g=const.
- Infall of unenriched gas Z_{in}=0
- Initial conditions $f_s(0)$=0, $Z(0)$=0
- if Z<<1

$$\frac{dZ}{df_s} = \frac{1}{f_g}\frac{y(1-R)\psi - ZR_{\text{in}}}{(1-R)\varphi} = \frac{y-Z}{f_g}$$

$$\frac{d(Z-y)}{df_s} = -\frac{1}{f_g}(Z-y)$$

$$Z = y\left[1-\exp\left(-\frac{f_s}{f_g}\right)\right] \rightarrow y \quad \text{as} \quad f_s \rightarrow \infty$$

Mean Stellar Metallicity

- Conservations of Metals

$$
\begin{aligned}
Z\, f_{\rm g} + Z_{\rm s}\, f_{\rm s} &= \int_0^t \int_{m'_t}^{m_u} p_{zm}\, \psi(t' - \tau_m)\, \phi(m)\; dm\, dt' \\
&= y(1-R) \int_0^\infty \psi\, dt \\
&= y(1-R)\, \frac{f_{\rm s}}{(1-R)} \\
&= y\, f_{\rm s}
\end{aligned}
$$

- Mean Stellar Metallicity

$$
Z_{\rm s} = y - \frac{f_{\rm g}}{1 - f_{\rm g}}
$$

- $Z_s \rightarrow y$ as $f_g \rightarrow 0$
- Metallicity Radial Gradients within galaxies
- Mass-Metallicity Relation of galaxies

Metallicity Distribution Functions

- $N(Z_1,Z_2)$: The number of stars with metallicity interval Z_1 to Z_2

$$N(Z_1,Z_2) = \int_{Z(t-\tau_m)=Z_1}^{Z(t-\tau_m)=Z_2} \int_{m_t}^{m_u} \psi(t-\tau_m)\frac{1}{m}\phi(m)dm\,dt$$

- **The G-dwarf Problem**: The observed number of metal-poor stars is smaller than in the closed-box model (e.g., Pagel 1975)
- Tinsley (1980)'s solutions: (1) Infall with ~5Gyr timescale, (2) pre-enrichment, (3) variable IMF, (4) metal-enhanced SF

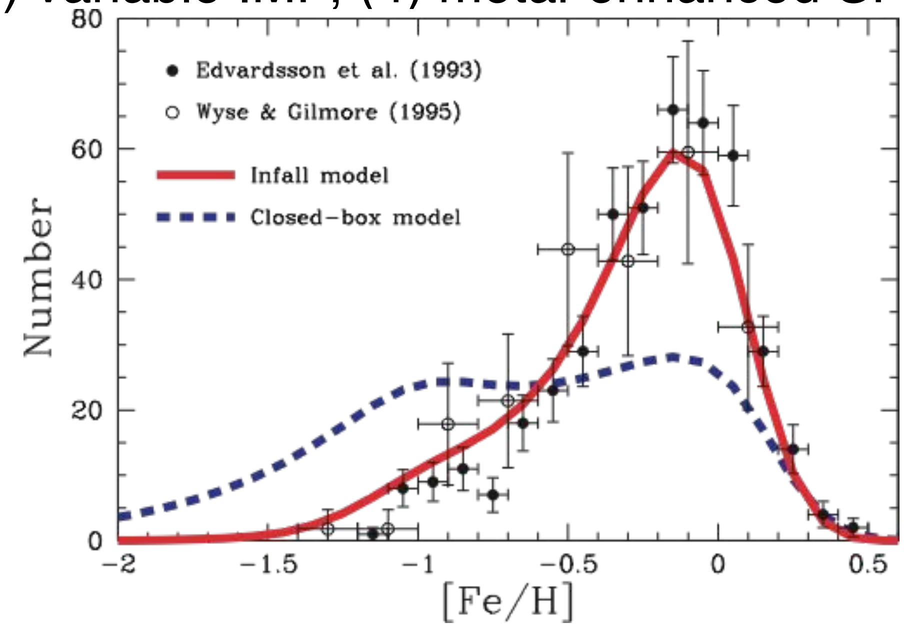

- The G-dwarf problem also exists in the bulge, ellipticals (Greggio 97), and dSphs (Helmi+06 but Starkenburg+10).

SNIa Model in GCE

CK et al. 1998, ApJ, 503, L155 on metallicity effect

CK & Nomoto 2009, 707, 1466

CK et al. 2015, ApJ, 804, 24 on subclasses of SNe Ia

also Greggio 2005, A&A, 441, 1055

Our SNIa progenitor model

Hachisu, Kato, Nomoto's binary calculation

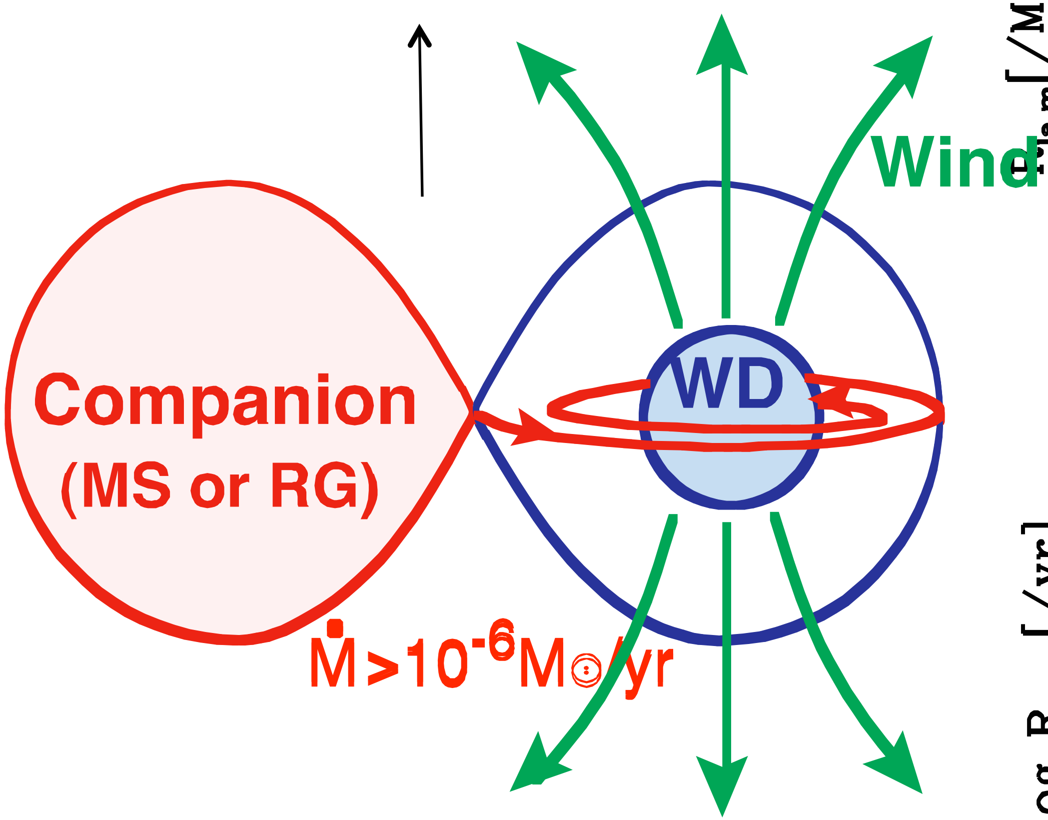

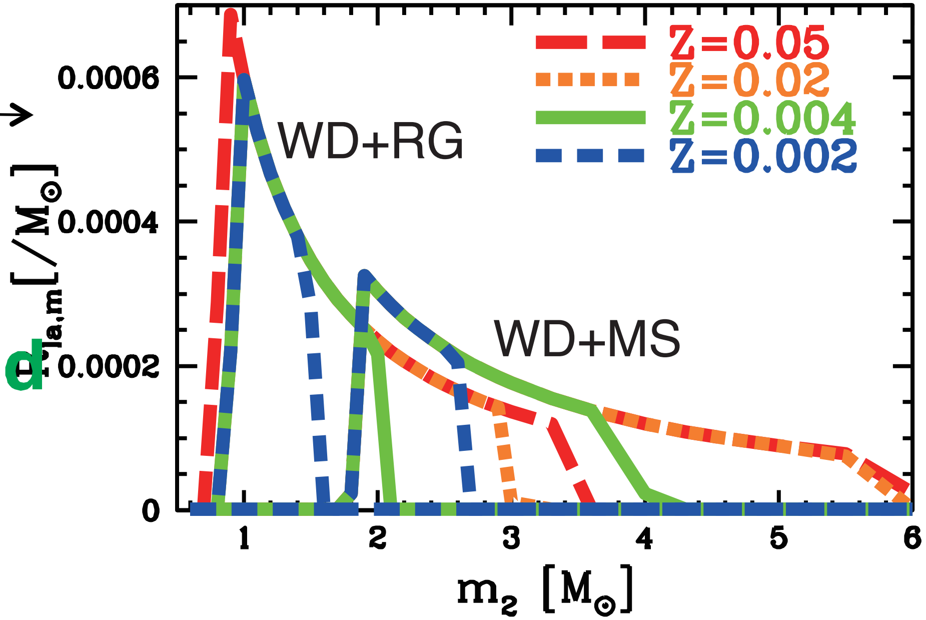

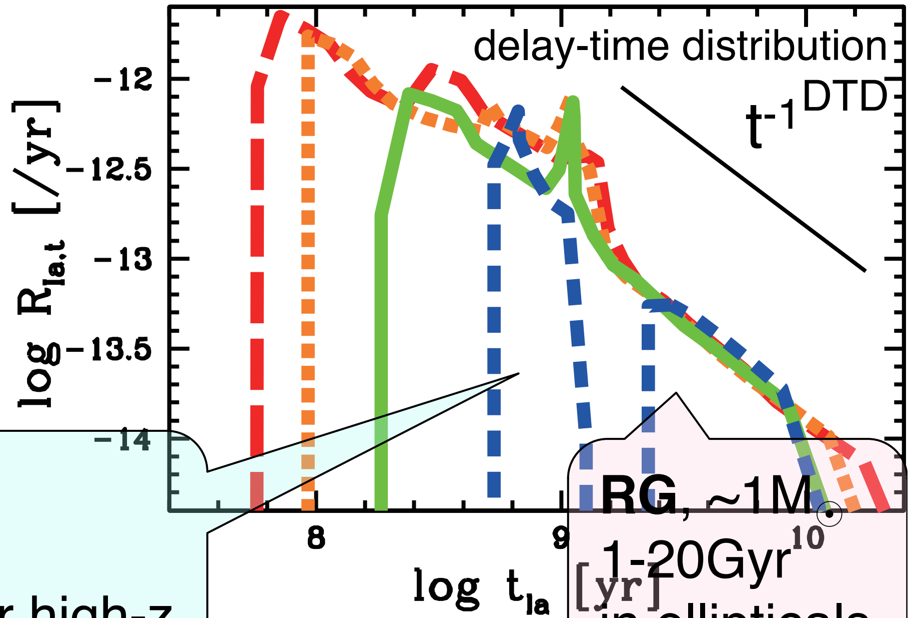

MS, ~3$M_\odot$
0.1-1Gyr
in spirals or high-z

RG, ~1$M_\odot$
1-20Gyr
in ellipticals

CK, Tsujimoto, et al. 98;
CK & Nomoto 09

Type Ia Supernovae

- Mass ejection,

$$E_{\rm Ia} = m_{\rm CO}\ \mathcal{R}_{\rm Ia}$$

- Metal ejection, Nucleosynthesis yields $p_{zm,\text{Ia}}$ (metallicity dependence included in CK2016)

$$E_{Z,\rm Ia} = m_{\rm CO}\ p_{zm,\rm Ia}\ \mathcal{R}_{Ia}$$

- SN Ia rate $\mathcal{R}_{\text{Ia}}$
  - Kobayashi et al. (1998)'s formula (random paring)

IMF of secondary star

$$\mathcal{R}_{\rm Ia} = b \left[\int_{\max[m_{\rm p,\ell},m_t]}^{m_{\rm p,u}} \frac{1}{m}\,\phi(m)\ dm\right]\left[\int_{\max[m_{\rm d,\ell},m_t]}^{m_{\rm d,u}} \frac{1}{m}\,\psi(t-\tau_m)\,\phi_{\rm d}(m)\ dm\right]$$

  - Greggio & Renzini (1983)'s formula

$$\mathcal{R}_{\rm Ia} = A\int_{\max[2m_2(t),m_{\rm B,\ell}]}^{m_2(t)+m_{\rm B,u}/2} \phi(m_{\rm B}) \left[\int_{\max[\frac{m_2(t)}{m_{\rm B}},\ \frac{m_{\rm B}-m_{\rm B,u}/2}{m_{\rm B}}]}^{0.5} \psi(t-\tau_{m_2})\,f(\mu)\,d\mu\right] dm_{\rm B}$$

IMF of total binary mass

mass fraction

binary mass ratio?

- Mass ratio $q=m_2/m_1$; mass fraction $\mu=m_2/(m_1+m_2)$

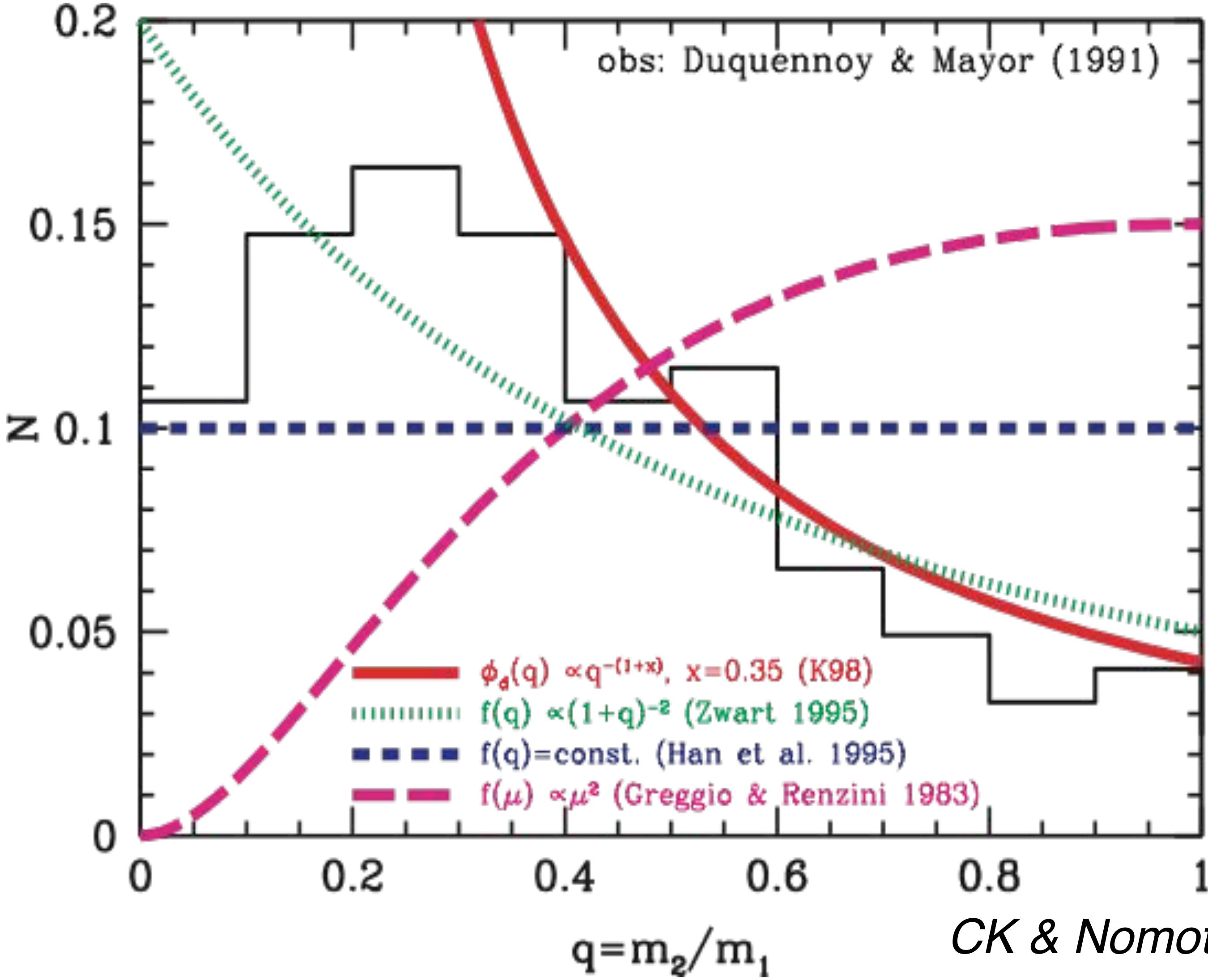

CK & Nomoto 2009

The Solar Neighborhood

to put a constraint on stellar physics (Step1)

CK, Umeda, Nomoto et al. 2006

CK, Karakas, Umeda 2011

Numerical Model for the solar neighborhood

- <u>Assumptions</u>
  - Salpeter IMF $0.07\text{-}50M_\odot$ or Kroupa IMF $0.01\text{-}50M_\odot$
  - Infall $R_{in} \propto t \exp(-t/\tau)$, τ=5Gyr, Z_{in}=0
  - SFR $\psi \propto f_g$, τ_s=2.2 or 4.7 Gyr
  - Initial f_g=f_s=0
  - Present f_g=0.15
  - Galactic Age = 13 Gyr

CK et al. 2011

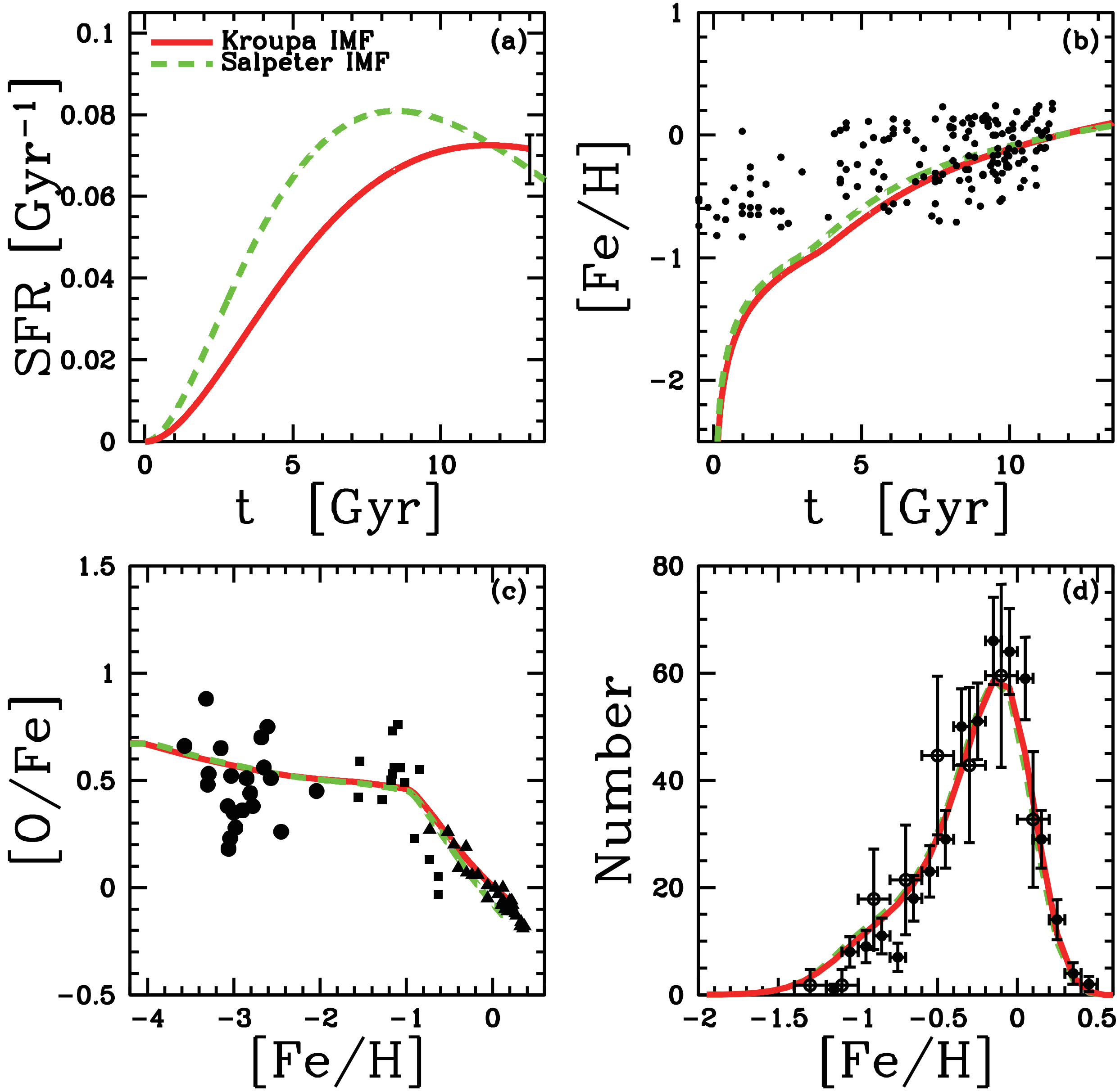

Numerical Model for the solar neighborhood

- **Assumptions**
  - Kroupa IMF $0.01\text{-}40M_\odot$
  - Infall $R_{in} \propto t \exp(-t/\tau)$, τ=5-8Gyr, Z_{in}=0
  - SFR $\psi \propto f_g$, τ_s=2-5 Gyr
  - Initial f_g=f_s=0
  - Present f_g=0.15
  - Galactic Age = 13 Gyr

CK et al. 2016

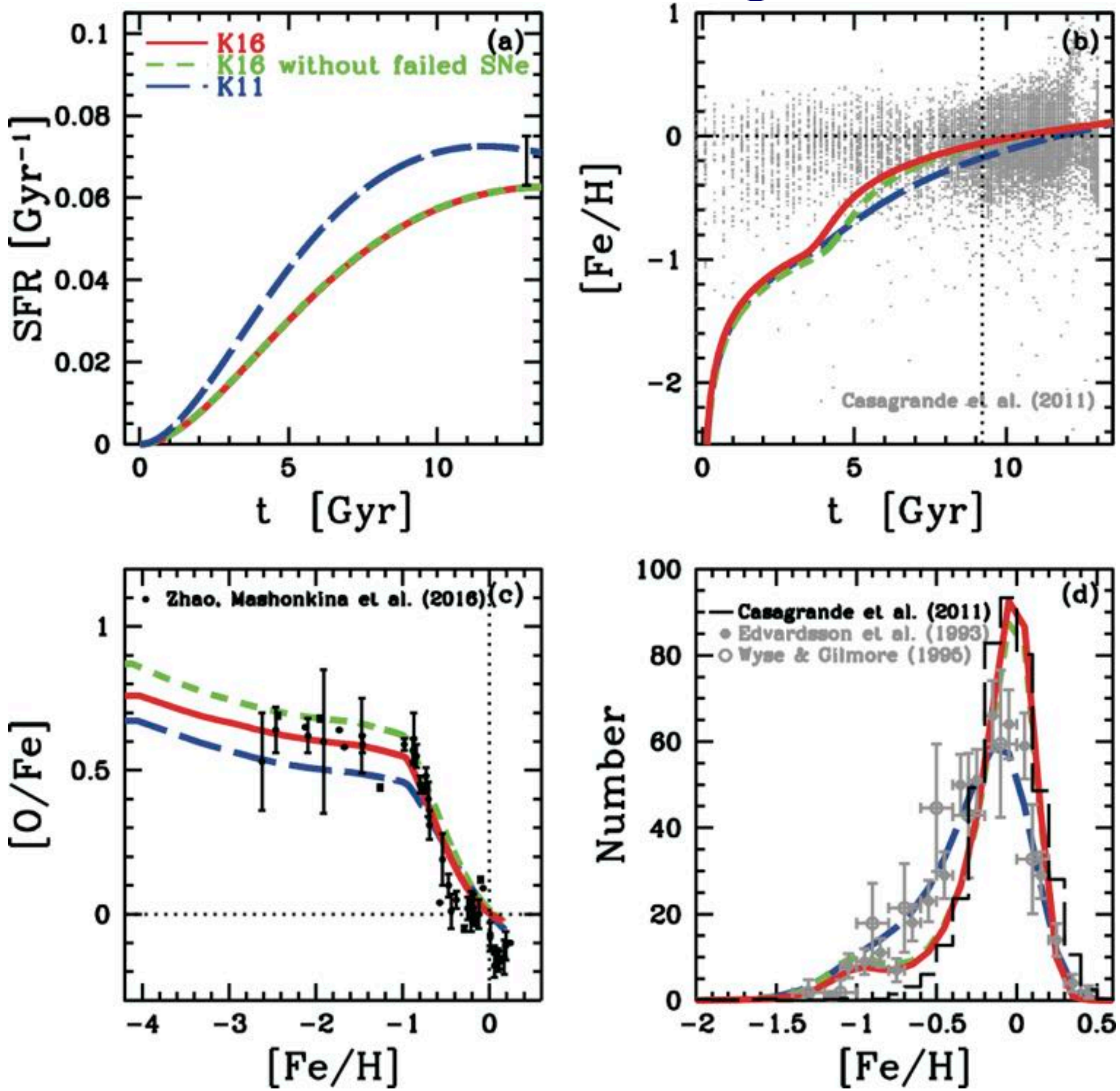

IMF dependence

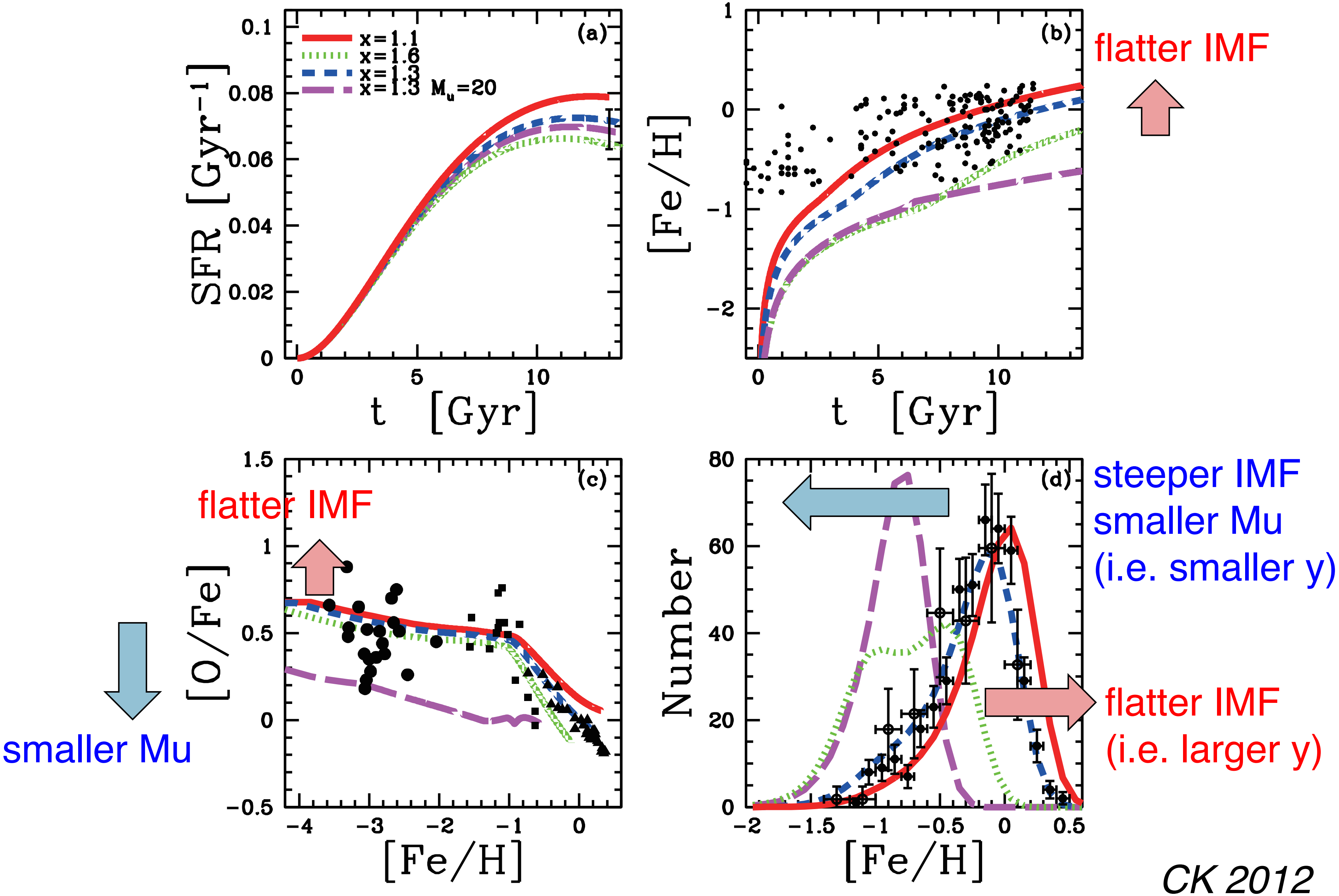

CK 2012

SFH dependence

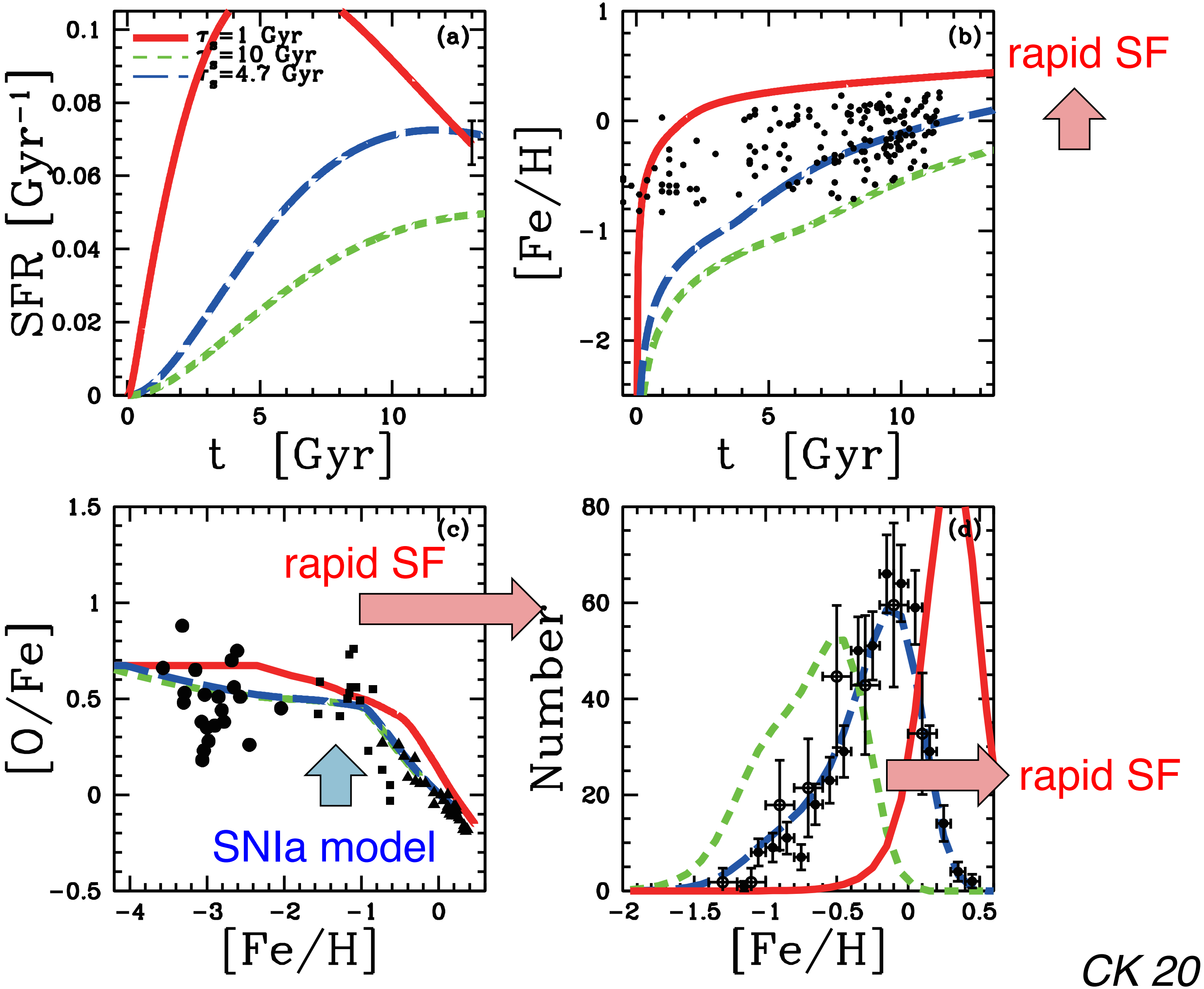

CK 2012

[X/Fe]-[Fe/H] relations

SN+HN+AGB (CK, Karakas, Umeda 2011), SN+HN; old SN yields only

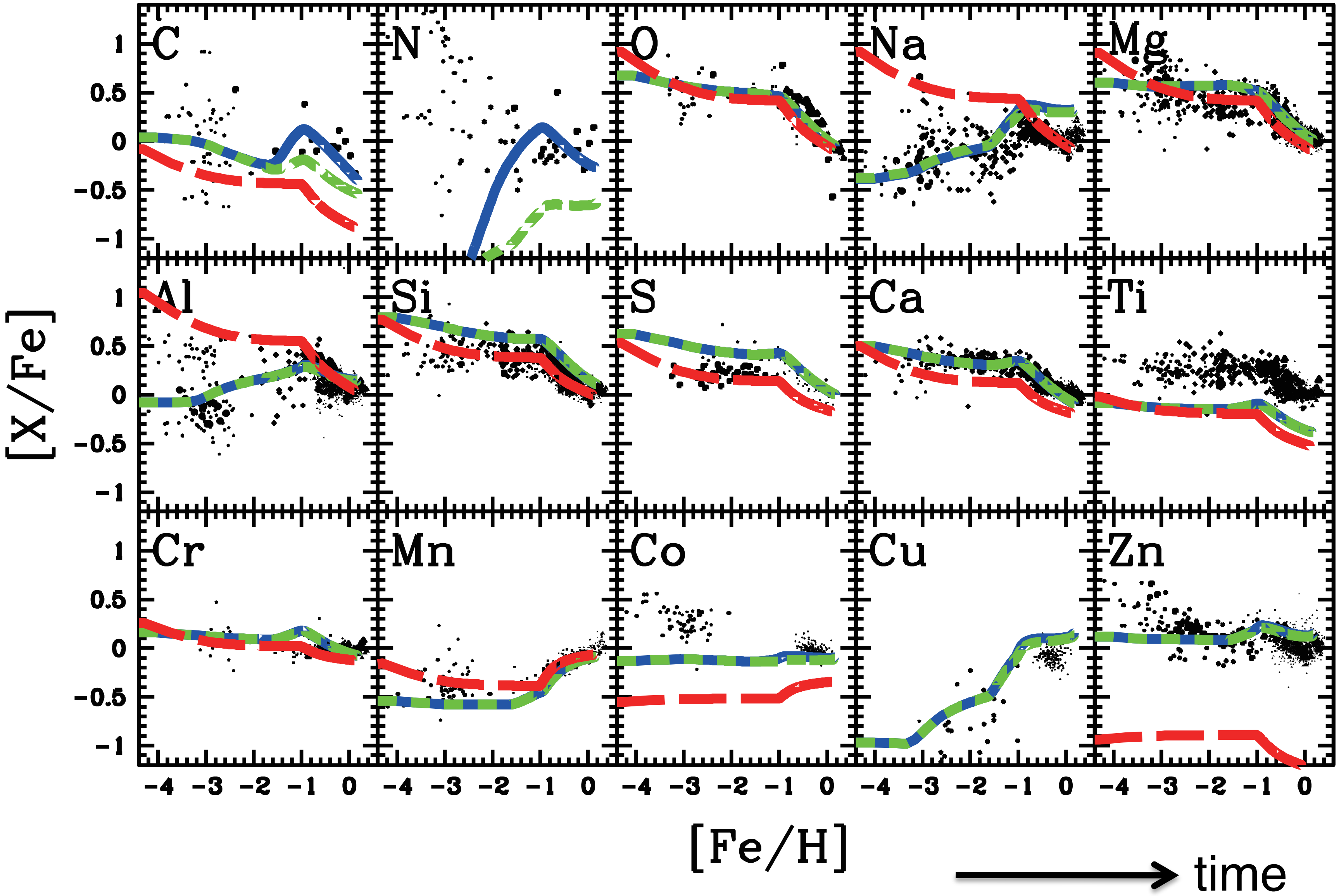

Elemental Abundances

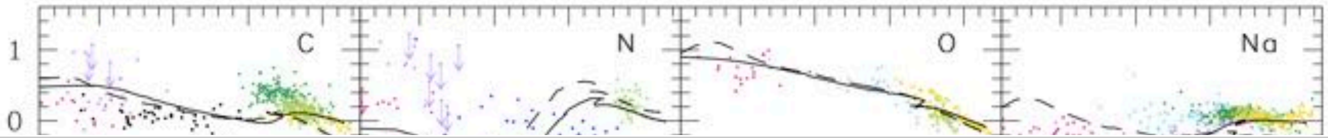

Model	Adopted stellar yields: LIMSs	Adopted stellar yields: Massive stars	Comments
1	vdHG97, $\eta_{\rm AGB}$ var	WW95, case B	Reference model
2	vdHG97, $\eta_{\rm AGB}$ var	WW95, case A	Mass cut changed
3	vdHG97, $\eta_{\rm AGB}$ var	WW95, case B + M92 pre-SN yields	Winds from $Z = Z_\odot$ massive stars included
4	vdHG97, $\eta_{\rm AGB}$ var	K06, $\varepsilon_{\rm HN} = 0$	SNII yields changed
5	vdHG97, $\eta_{\rm AGB}$ var	K06, $\varepsilon_{\rm HN} = 1$	HN nucleosynthesis included
6	vdHG97, $\eta_{\rm AGB}$ var	K06, $\varepsilon_{\rm HN} = 1$ + Geneva pre-SN yields, $\upsilon_{\rm ini} \neq 0$	Stellar rotation included
7	vdHG97, $\eta_{\rm AGB}$ var	K06, $\varepsilon_{\rm HN} = 1$ + Geneva pre-SN yields, $\upsilon_{\rm ini} = 0$	
8	vdHG97, $\eta_{\rm AGB}$ const	K06, $\varepsilon_{\rm HN} = 1$ + Geneva pre-SN yields, $\upsilon_{\rm ini} \neq 0$	Mass loss along the AGB changed
9	vdHG97, minimum HBB	K06, $\varepsilon_{\rm HN} = 1$ + Geneva pre-SN yields, $\upsilon_{\rm ini} \neq 0$	HBB extent reduced
10	M01, $\alpha = 1.68$	K06, $\varepsilon_{\rm HN} = 1$ + Geneva pre-SN yields, $\upsilon_{\rm ini} \neq 0$	LIMS yields changed
11	M01, $\alpha = 2.50$	K06, $\varepsilon_{\rm HN} = 1$ + Geneva pre-SN yields, $\upsilon_{\rm ini} \neq 0$	HBB strength increased
12	M01, $\alpha = 1.68$	K06, $\varepsilon_{\rm HN} = 1$ + [Geneva, $\upsilon_{\rm ini} \neq 0$ + M92] pre-SN yields	
13	KL07, with extra pulses	K06, $\varepsilon_{\rm HN} = 1$ + Geneva pre-SN yields, $\upsilon_{\rm ini} \neq 0$	AGB yields from detailed stellar models
14	KL07, with extra pulses	K06, $\varepsilon_{\rm HN} = 1$ + [Geneva, $\upsilon_{\rm ini} \neq 0$ + M92] pre-SN yields	
15	K10, without extra pulses	K06, $\varepsilon_{\rm HN} = 1$ + Geneva pre-SN yields, $\upsilon_{\rm ini} \neq 0$	Up-to-date nuclear reaction rates for LIMSs

Notes. vdHG97: van den Hoek & Groenewegen (1997); WW95: Woosley & Weaver (1995); M92: Maeder (1992); K06: Kobayashi et al. (2006); M01: Marigo (2001); KL07: Karakas & Lattanzio (2007); K10: Karakas (2010). The models adopting the yields by Marigo (2001) for LIMSs use self-consistent nucleosynthesis prescriptions from Portinari et al. (1998) for stars of initial mass $m = 6\ M_\odot$ and $m = 7\ M_\odot$.

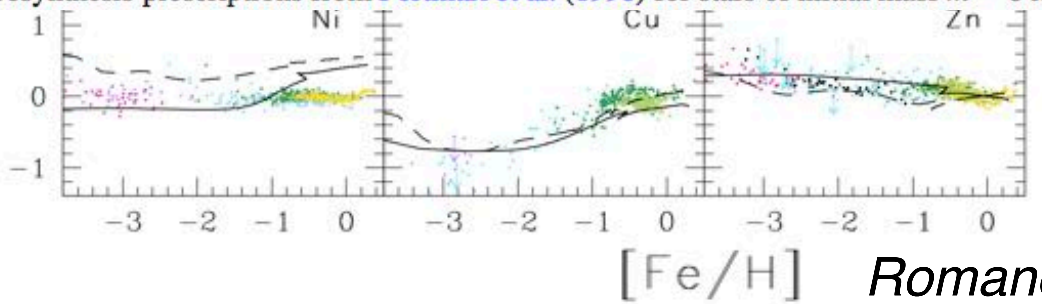

Romano, et al, Matteucci 2010

Fig. 22. [X/Fe] versus [Fe/H] relations for elements from C to Zn in the solar neighbourhood. The predictions from Models 1 and 15 (dashed and solid curves, respectively) are compared to data from several sources (see captions to Figs. 3 to 16 for references).

Isotope Ratios

CK, Karakas, Umeda (2011)

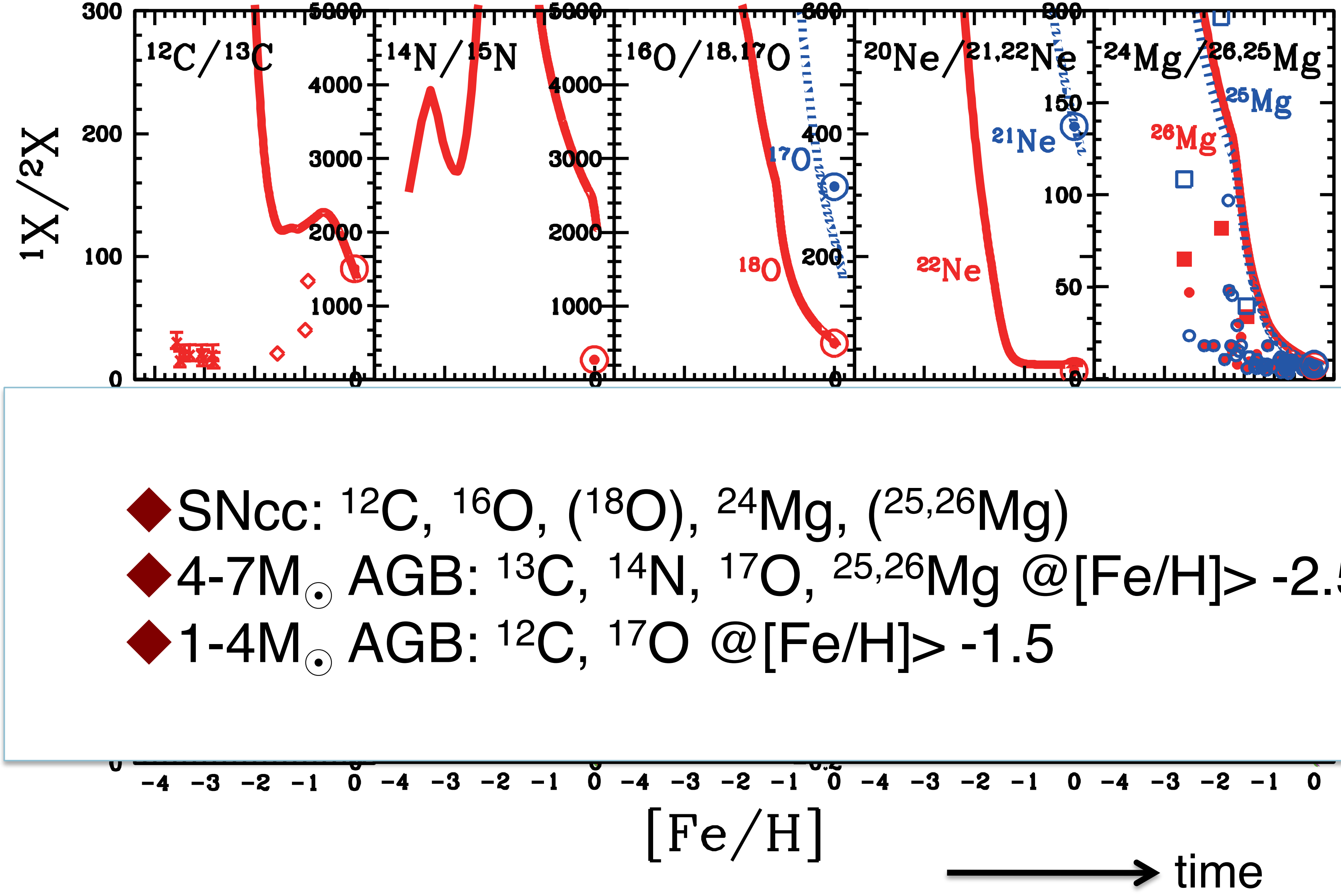

- SNcc: ^{12}C, ^{16}O, (^{18}O), ^{24}Mg, ($^{25,26}Mg$)
- 4-7$M_\odot$ AGB: ^{13}C, ^{14}N, ^{17}O, $^{25,26}Mg$ @[Fe/H]> -2.5
- 1-4$M_\odot$ AGB: ^{12}C, ^{17}O @[Fe/H]> -1.5

Isotope Ratios

CK, Karakas, Umeda (2011)

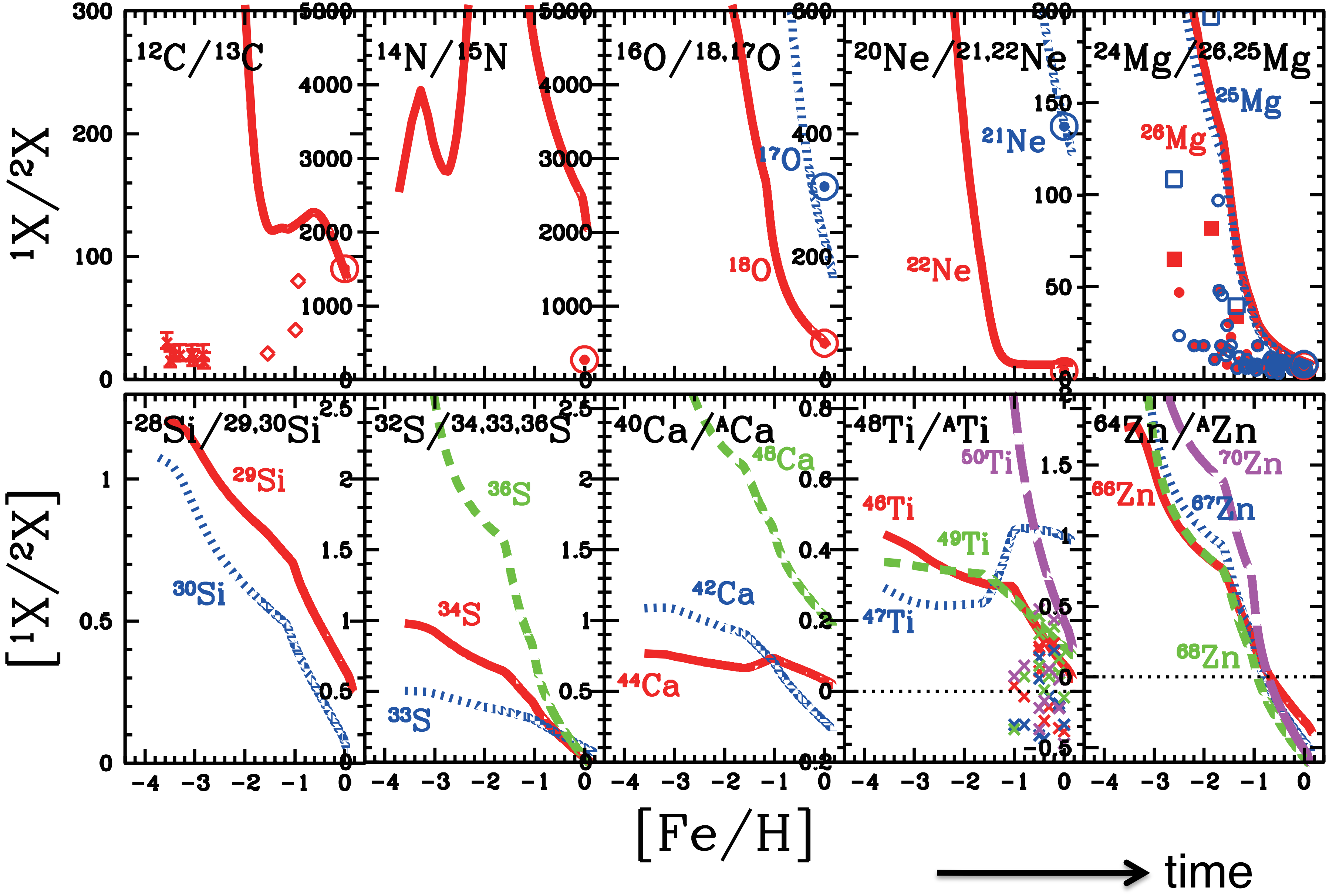

ν process

- Use Umeda & Nomoto's progenitor star models with $M=15,25,50M_{\odot}$, Z=0, 0.004, 0.02, E=1 and (1,10,40) $\times 10^{51}$ erg
- Calculate nucleosynthesis
- assuming time-dependent ν emission
  - Total ν luminosity $E_{\nu}=3$ or 9×10^{53} erg
  - Fermi-Dirac distribution of energy spectra
  - ν temperature T_{ν} = 6 MeV/k for $\nu_{\mu},\nu_{\mu},\nu_{\tau},\nu_{\tau}$, 4 Mev/k for ν_{e}, ν_{e}
  - exponential decay with a timescale of 3 sec
- Neutral current reactions

$$\begin{aligned}(Z,A)+\nu \rightarrow (Z,A)^{*}+\nu' &\rightarrow (Z,A-1)+n+\nu' \qquad (1)\\ &\rightarrow (Z-1,A-1)+p+\nu' (2)\\ &\rightarrow (Z-2,A-4)+\alpha+\nu' (3)\end{aligned}$$

- Charged current reactions
  - $(Z,A)\rightarrow(Z-1,A)$ or $(Z+1,A)$

F, K, Sc, (Ti), V

The Fluorine Problem

CK, Izutani, Karakas, T.Yoshida, Yong, Umeda 2011

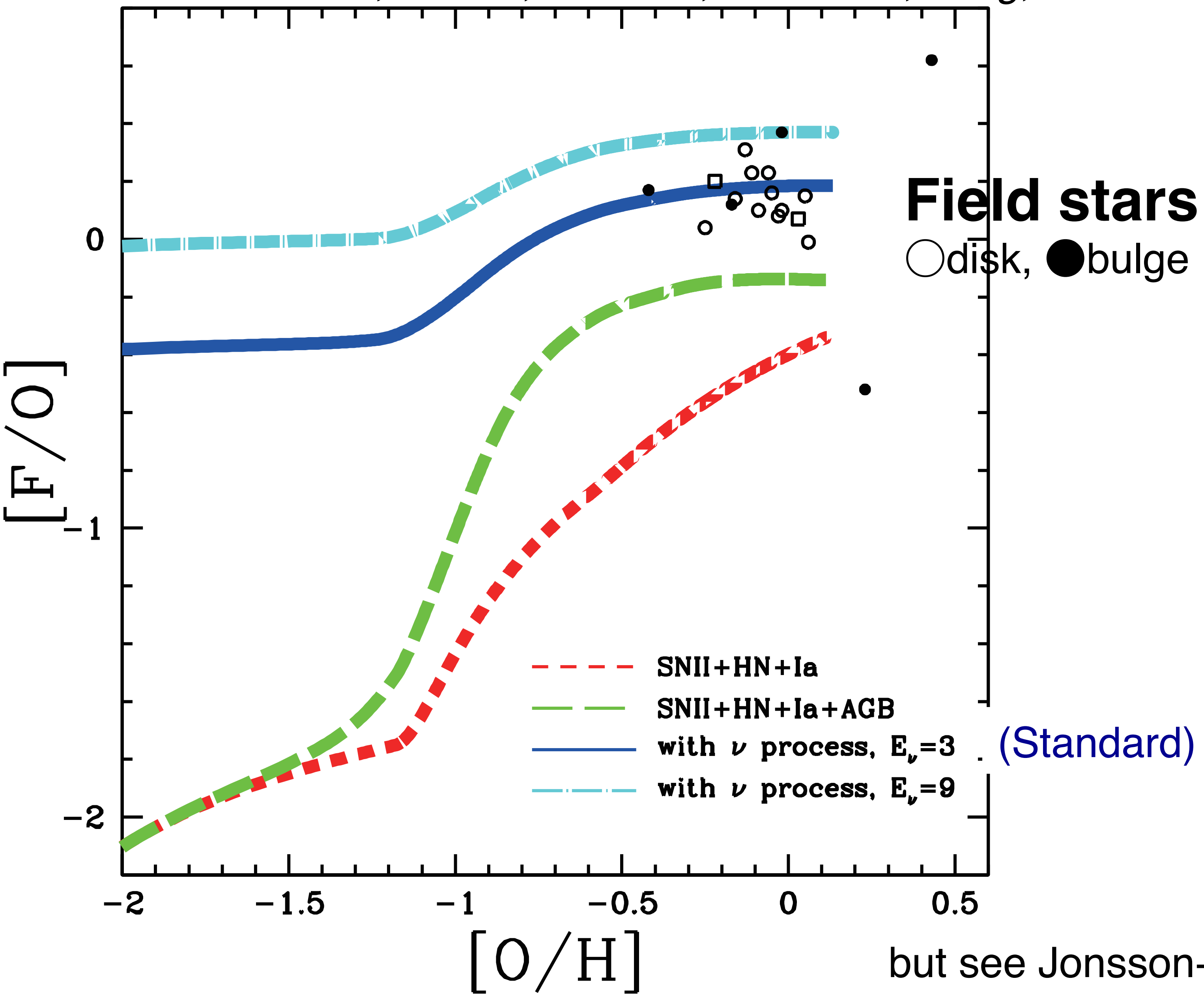

but see Jonsson+ 14

2D effect

- ✷ Hypernova (>20M$_\odot$, >10^{51} erg) is evidenced from observed nearby SNe. The mechanism is not known.
- ✷ Nucleosynthesis of (artificial) jet +2D hydro calculated (Maeda & Nomoto 03; Tominaga 09)

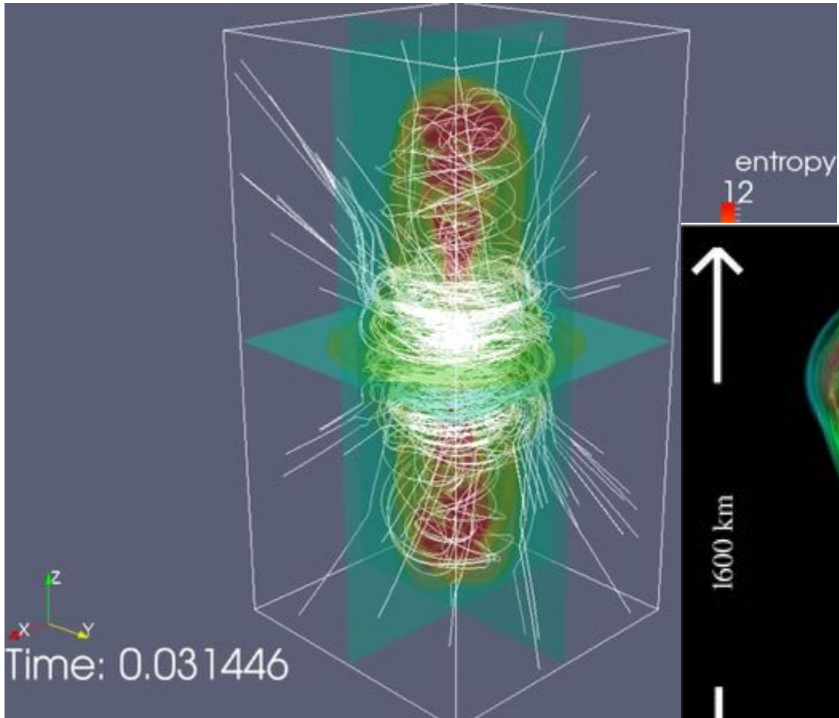

←Winteler+12, 15M$_\odot$, 5x10^{12} G
r-process with tracer particles

↓GRMHD: Mösta+14, 25M$_\odot$, 10^{12} G

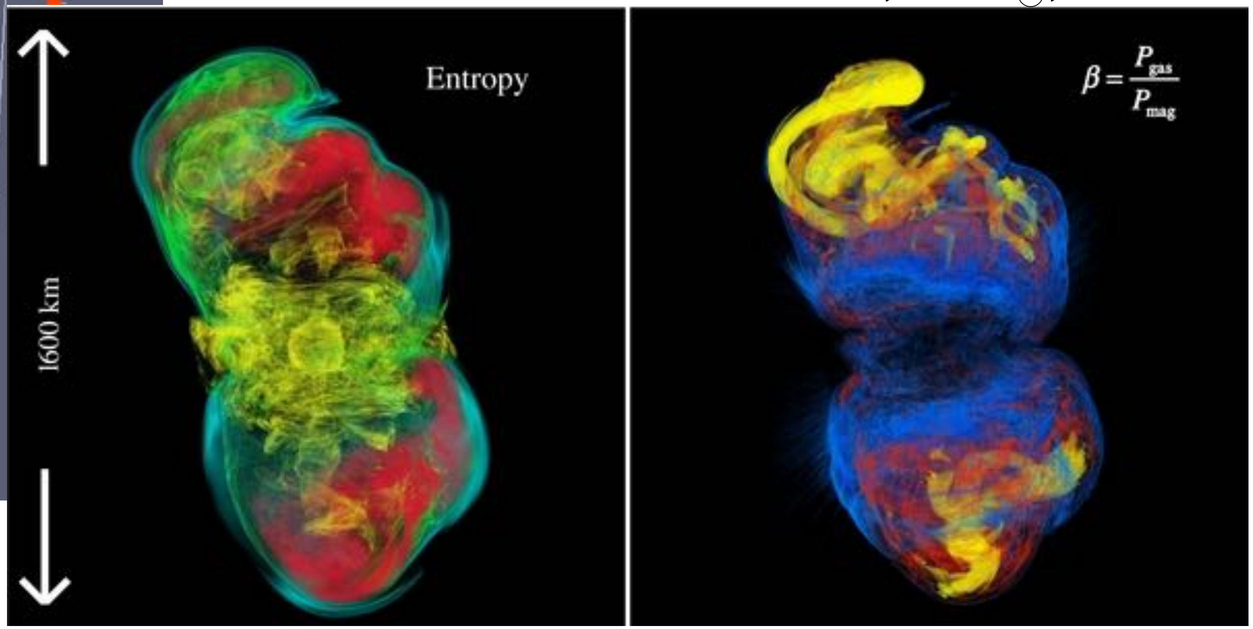

Sneden, Cowan, CK, et al 2016

K06: GCE model w Salpeter IMF

K11: GCE model w Kroupa IMF

K15: HN with 2D jet effects, SNIa yields of delay.det.

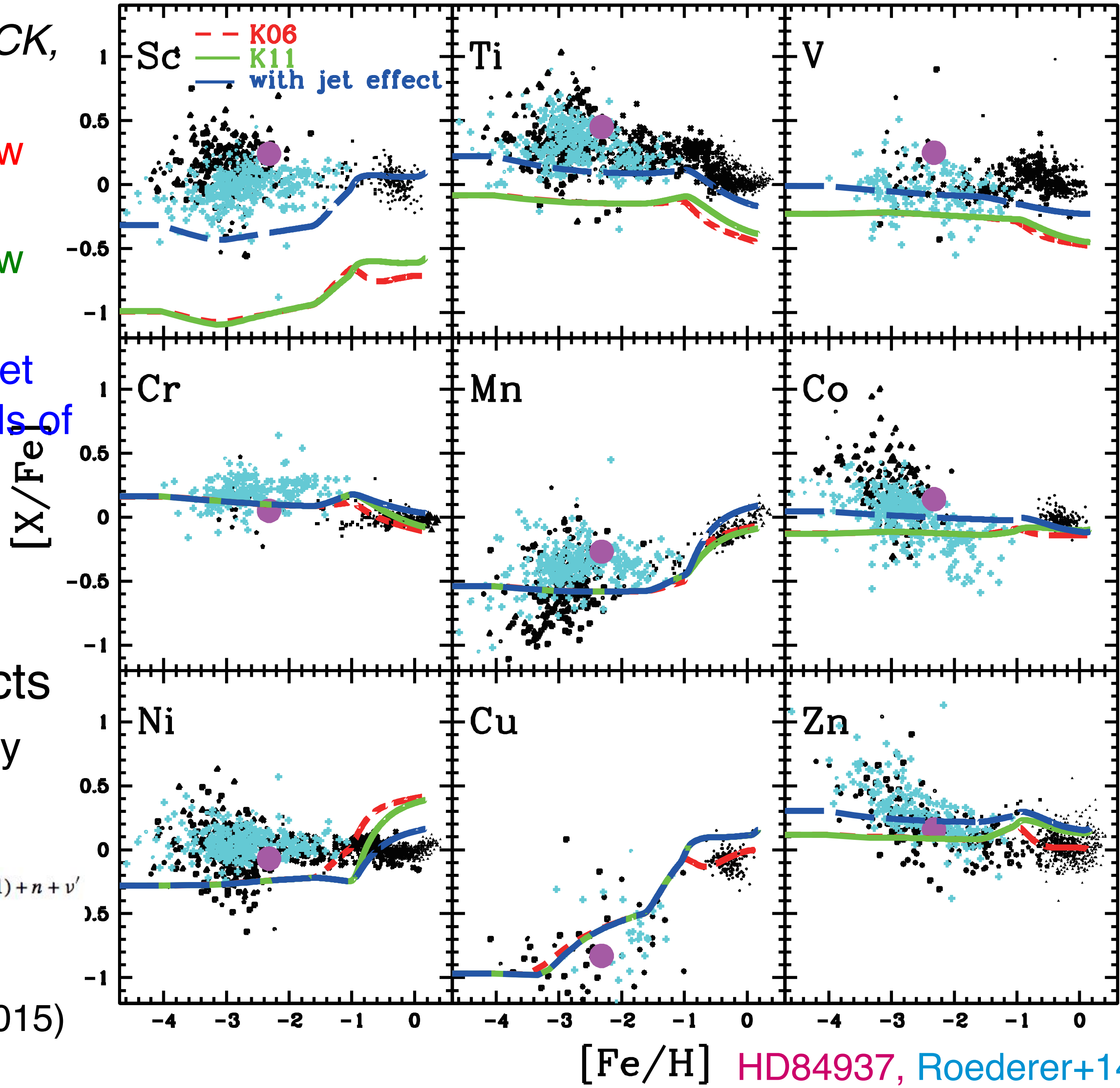

Importance of

- 2D (jet) effects
  - high entropy
- ν-process

$$(Z, A) + \nu \rightarrow (Z, A)^* + \nu' \rightarrow (Z, A-1) + n + \nu'$$
$$\rightarrow (Z-1, A-1) + p + \nu'$$
$$\rightarrow (Z-2, A-4) + \alpha + \nu'.$$

(CK, Izutani, et a. 2015)

HD84937, Roederer+14

Super AGB & ECSN

Doherty +15

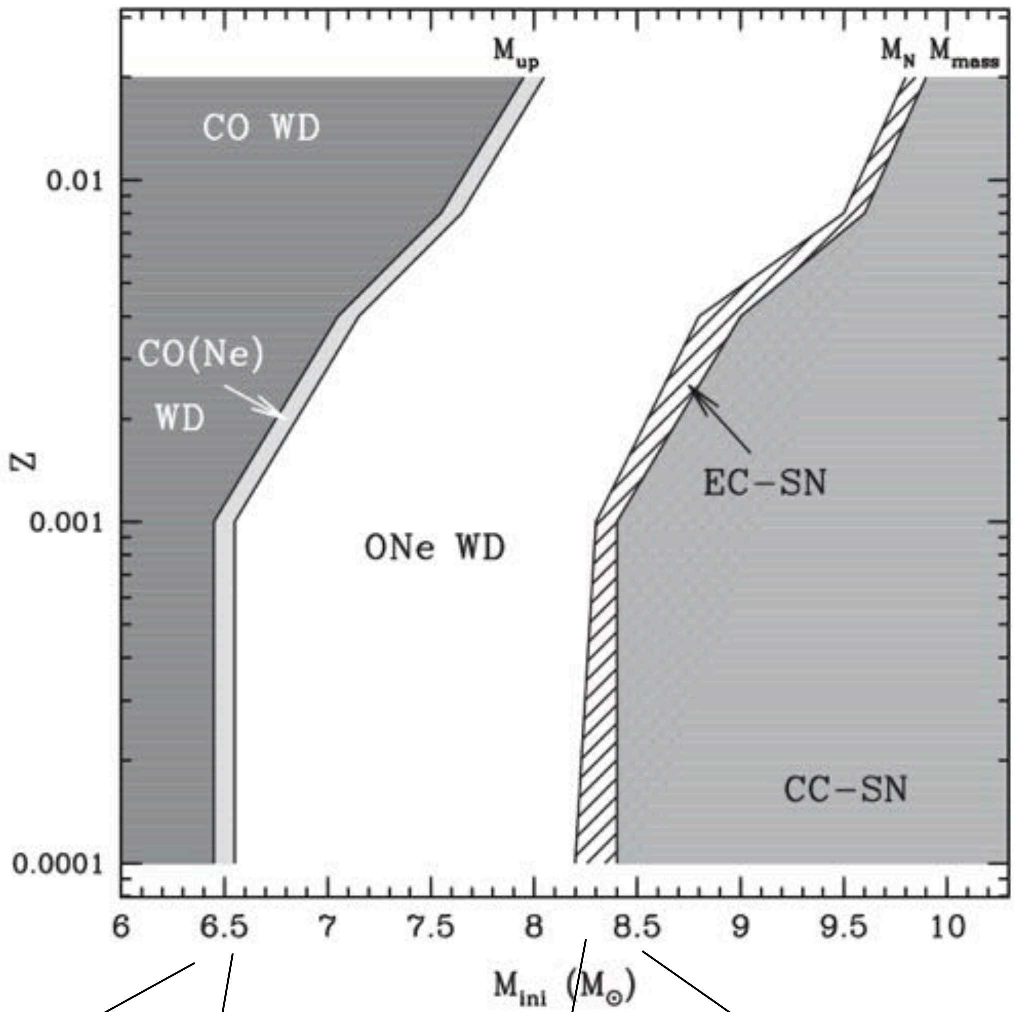

Karakas 10 Fink+14 Doherty+14 Wanajo+09 CK+06,11(=NKT13)

8-10$M_\odot$ stars don't contribute <Zn

SN+HN+AGB+SNIa(Z), SAGB, ECSN, Iax

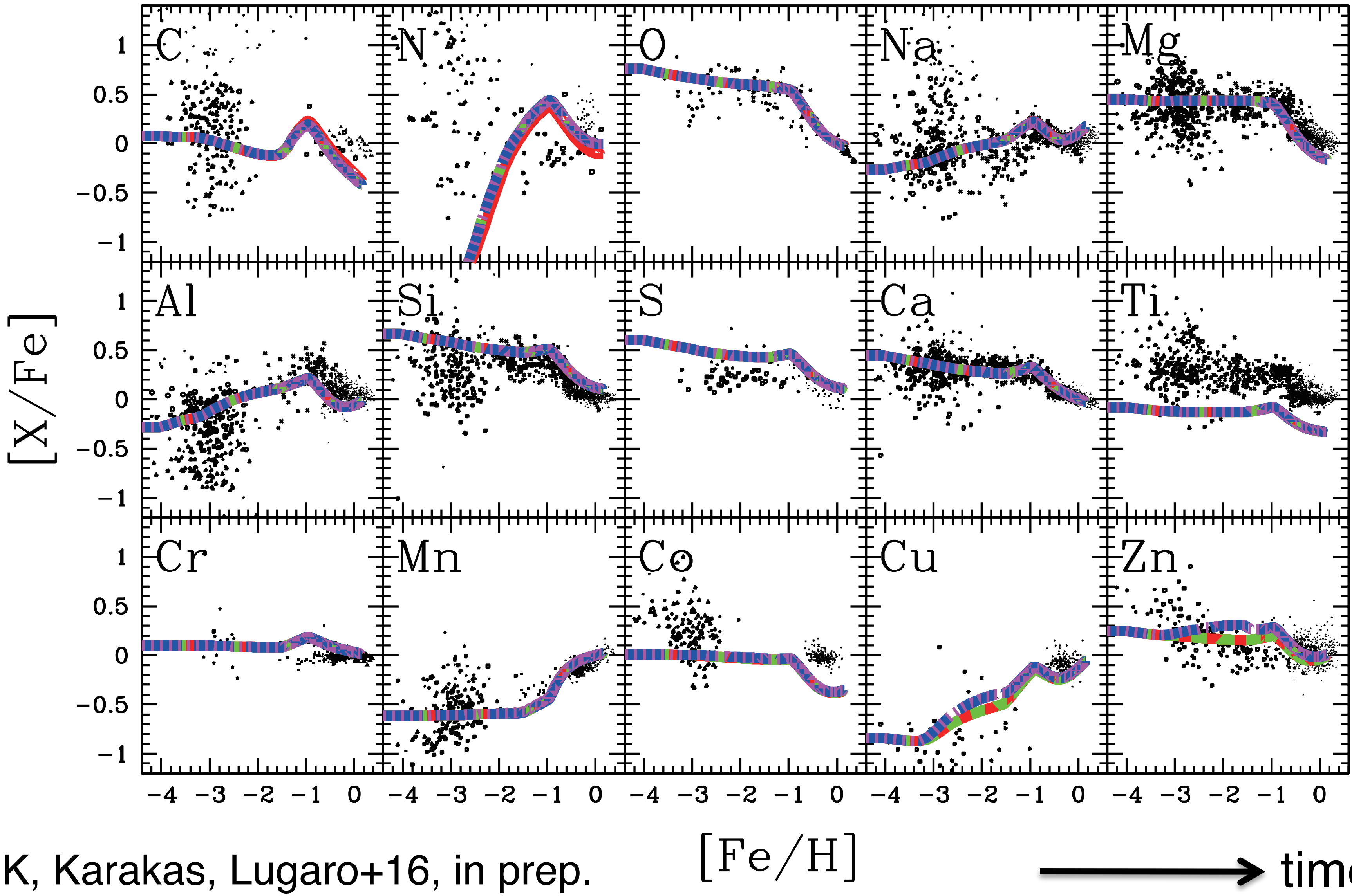

CK, Karakas, Lugaro+16, in prep.

time

Chemical Evolution in dSphs

CK, Nomoto, Hachisu 2015, ApJL, 804, 24

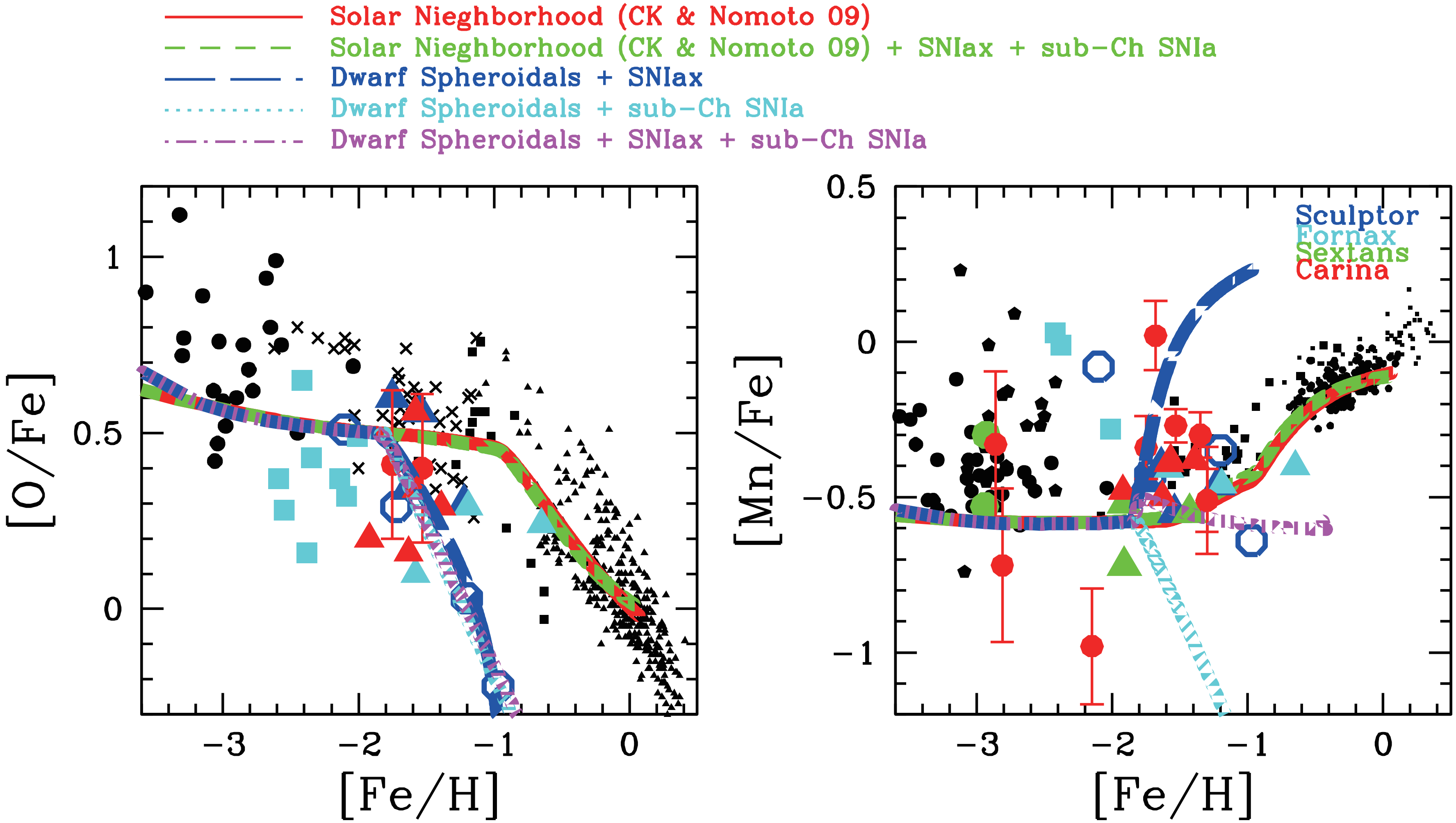

- ✷ In deflagrations, Mn is mostly synthesized in NSE, while in sub-Ch SNeIa, mostly in incomplete-Si burning, which depends on Z.
- ✷ A mix of sub-Ch SNIa & SNIax can reproduce [Mn/Fe]~ -0.5.

Failed Supernovae >20M$_\odot$

Smartt (2099), ARAA

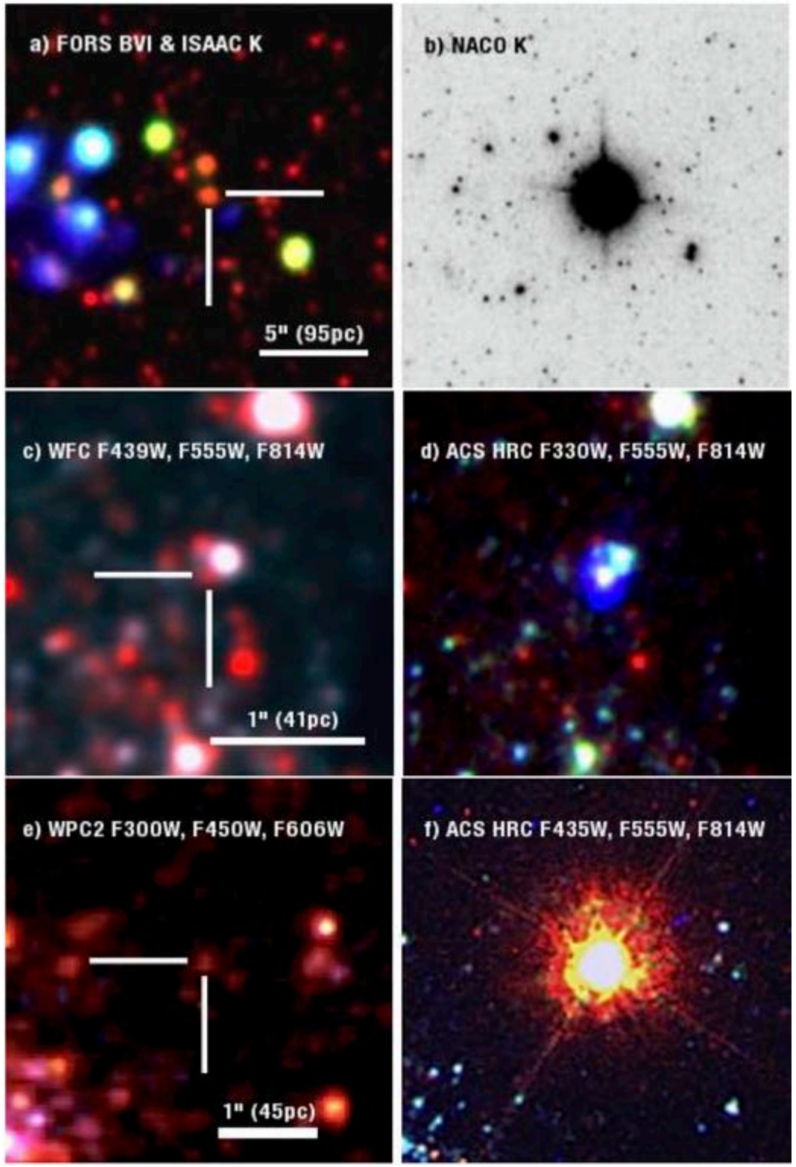

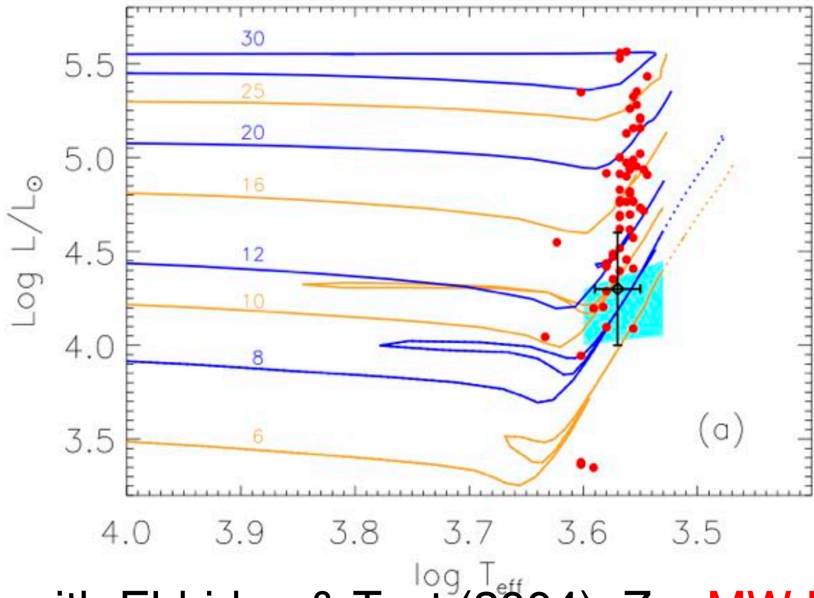

with Eldridge & Tout (2004), Z$_\odot$, MW RSGs

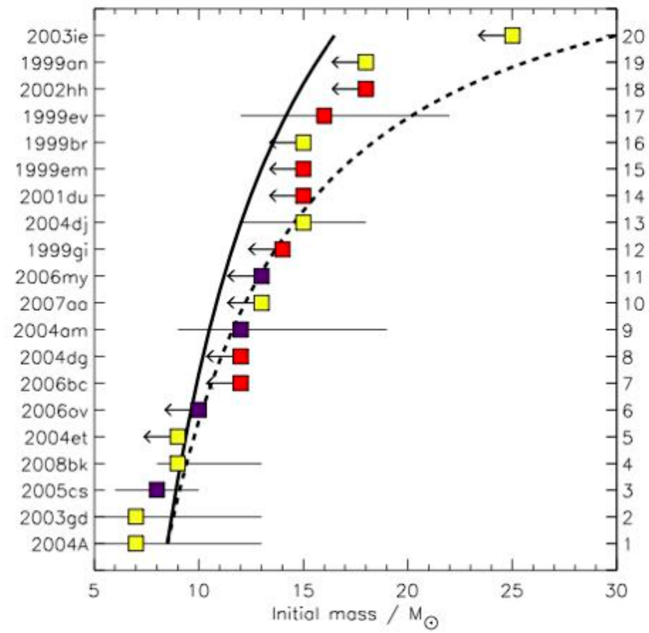

Failed SNII (>25M$_\odot$) with HN✔

SN+HN+AGB+SNIa(Z), Failed SN, w/o HN, Failed SN w HN

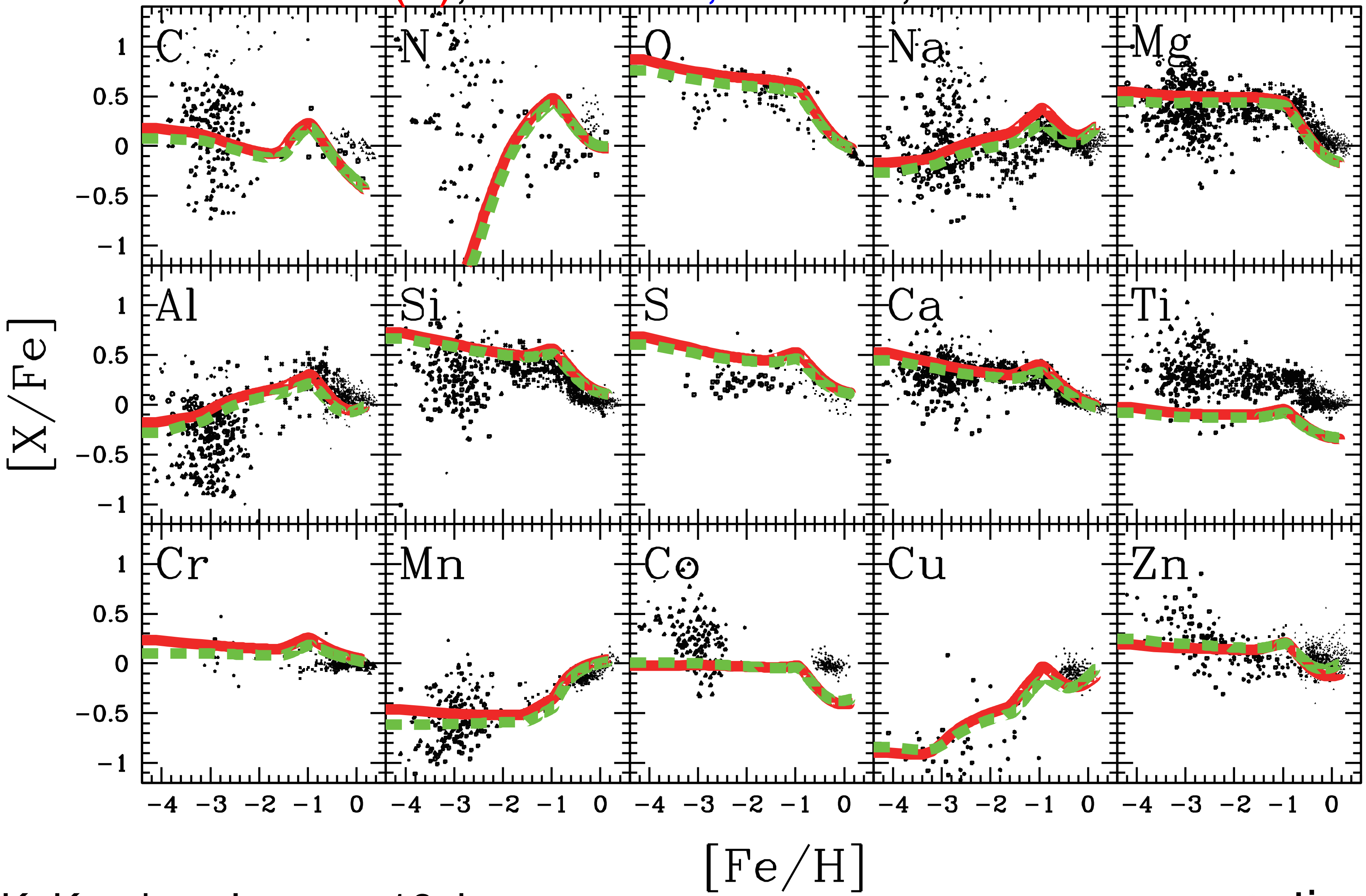

CK, Karakas, Lugaro+16, in prep.

time

The Milky Way Galaxy

to put a constraint on the star formation history (Step2)

The Milky Way Galaxy

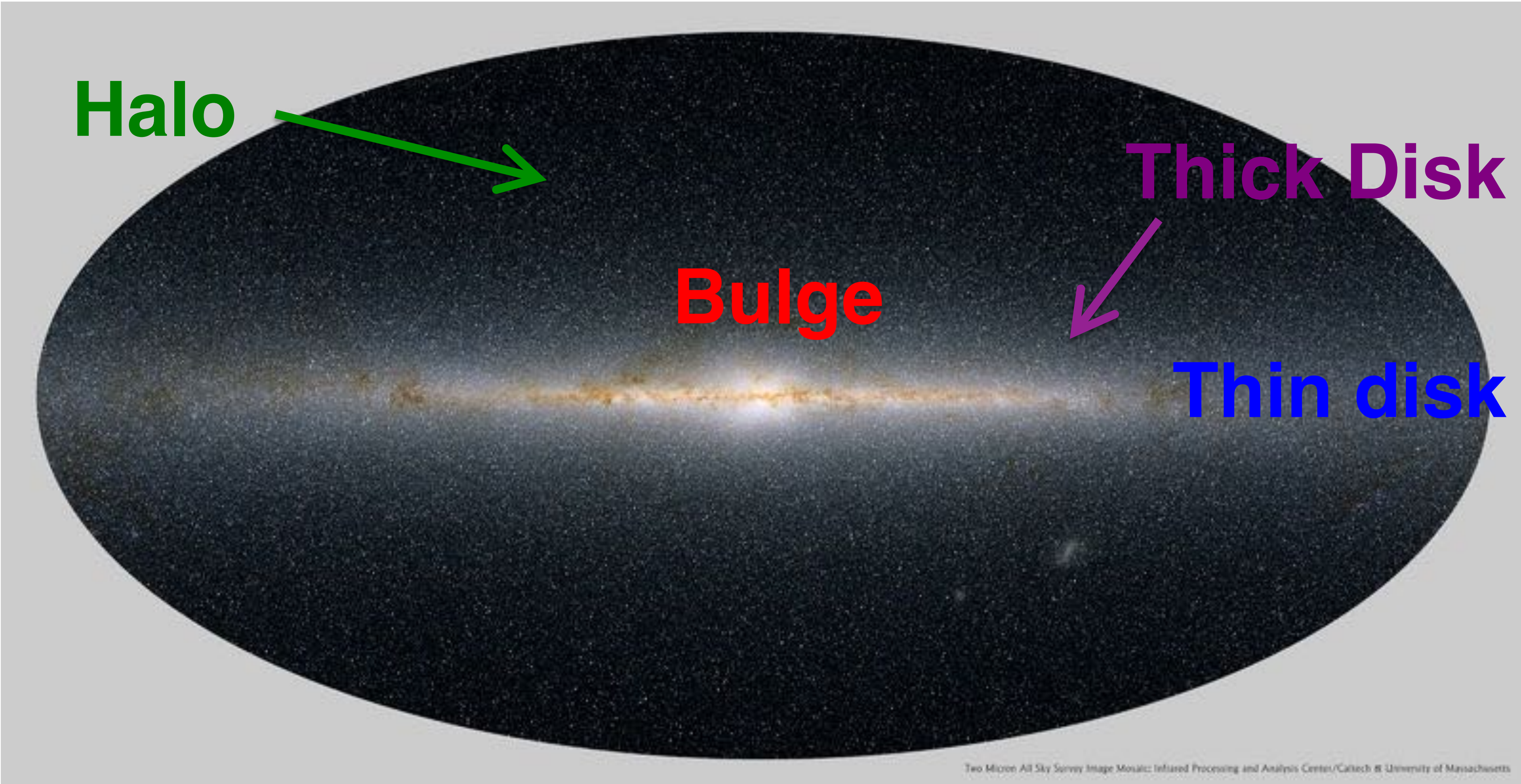

The Origin of Milky Way Galaxy

sec 7.2-7.4, NKT13, ARAA; reference incomplete

- **Disk** **(**Pilkington+12**)** – Radial gradients at higher-z
  - **Inside-out** (chemodynamical sim.): flat
  - **Monolithic collapse**: flat/inverse (Chiappini), flat/steep (*Molla*)
  - **Migration**: ? (Schönrich & Binney 09), Minchev
- **Bulge**
  - **Classical** (cosmological sim., assembly of gas-rich dwarfs): slightly different from thick disk, vertical gradient ✓
  - **Pseudo** (**bar-driven, secular evolution**): boxy bulges (e.g., Athanassoula & Misiriotis 2002) with cylindrical rotation ✓
- **Thick Disk** stars
  - **Minor mergers/accretion** (cosmological sim.): lower [Fe/H] than bulge ✓
  - **Radial mixing**: [O/Fe] ✓ (Schönrich & Binney 09)
  - **Disk heating:** vertical gradient ? (Villalobos & Helmi 08)
  - **Clumpy disk**: constant scale height with radius (Bournaud, Elmegreen+09) ✖

Pseudo-bulge etc

Shen et al. 2010

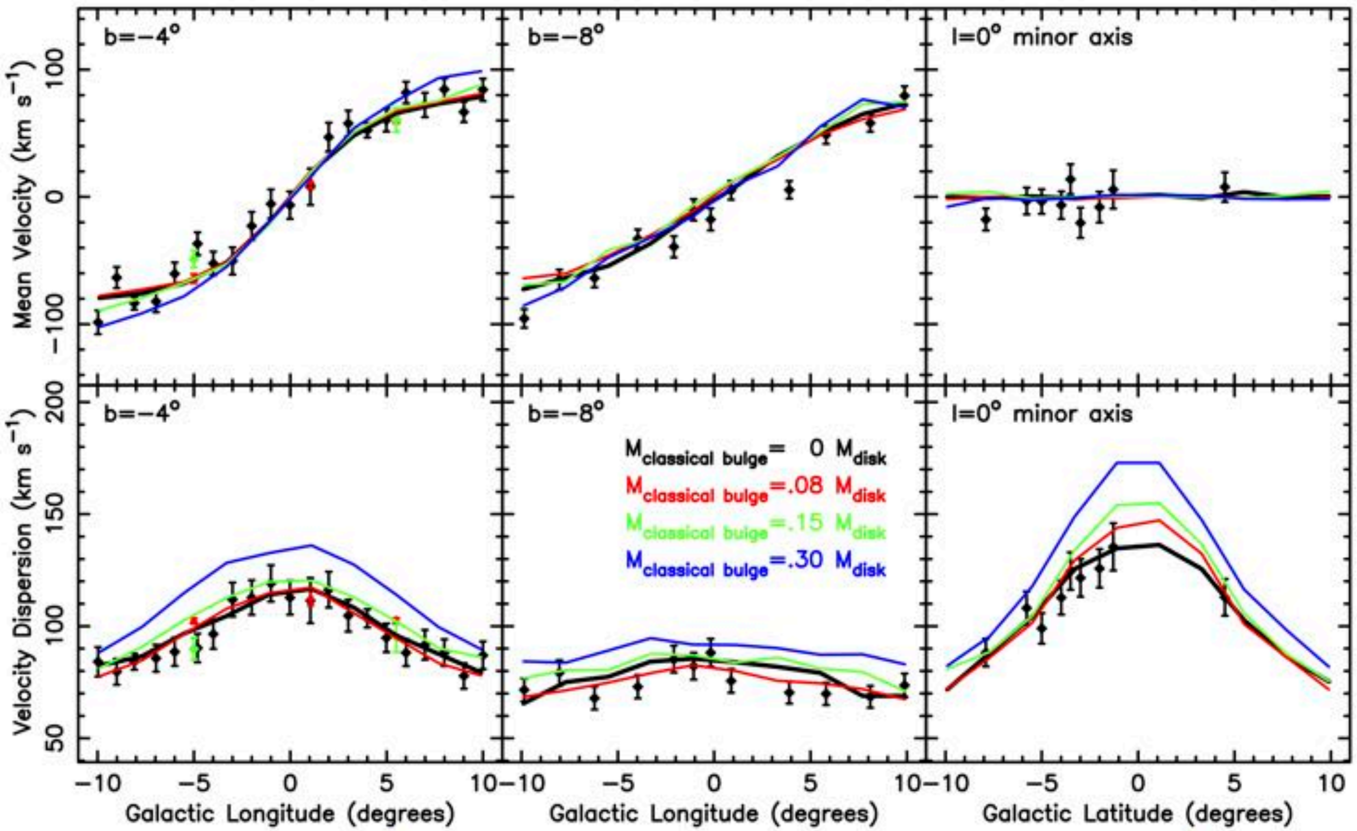

Figure 4. Fits to the kinematic data (cf. Figure 2) of models that include a pre-existing classical bulge. The heavy black lines from Figure 2 represent the model without a classical bulge. The red, green, and blue lines are for models whose classical bulges have masses of 8%, 15%, and 30%, respectively, of the disk mass $M_{\rm disk}$. Including a classical bulge significantly worsens the model fits to the data, especially along the minor axis.

- ✷ Cosmological simulations with high resolution could form this (Athanassoula, Scannapieco)
- ✷ Secular evolution can have vertical gradient (Martinez-Valpuesta & Gerhard 13) if initial disk had radial gradient

[X/Fe] can constrain SFH?

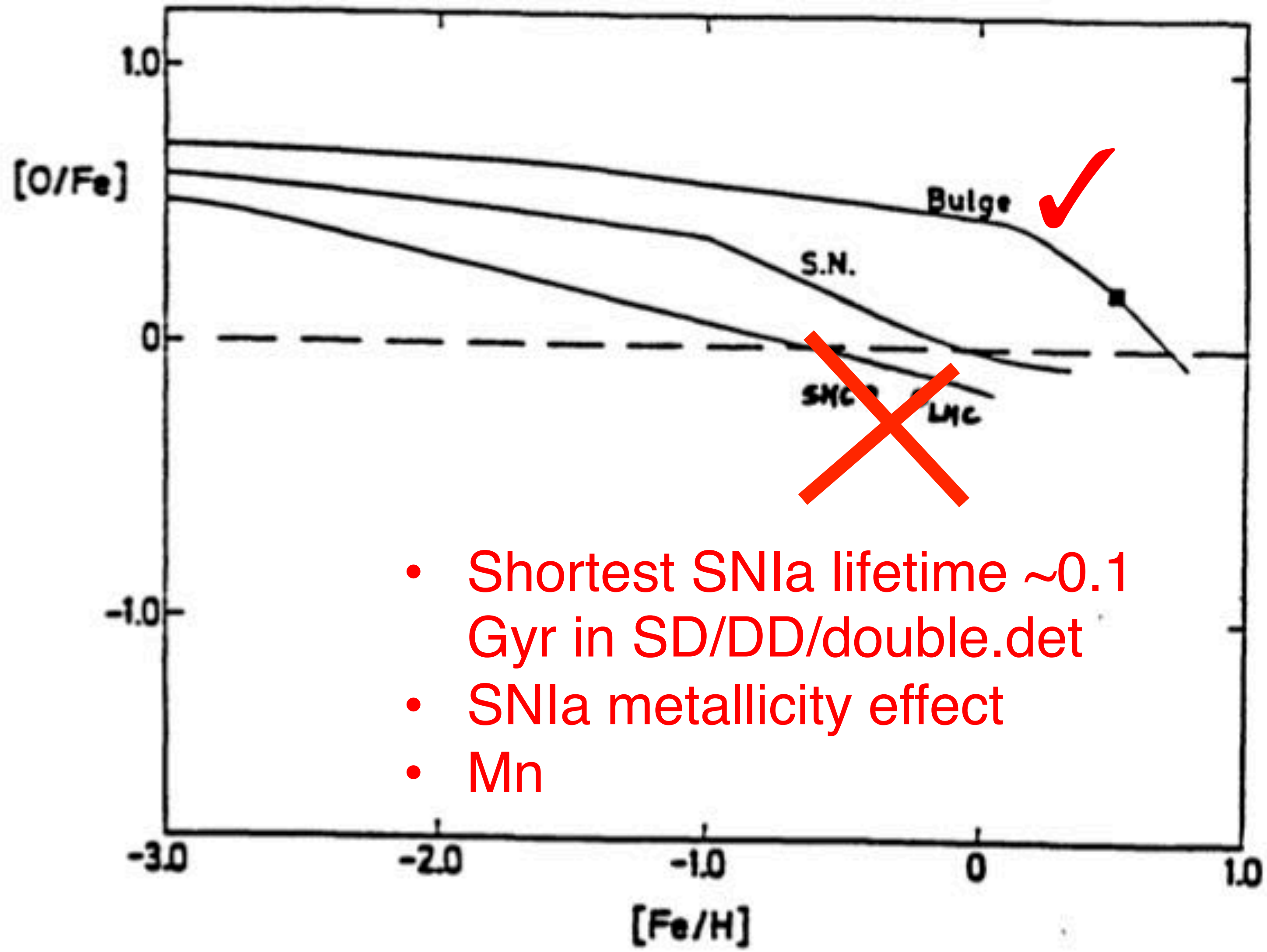

- Shortest SNIa lifetime ~0.1 Gyr in SD/DD/double.det
- SNIa metallicity effect
- Mn

Matteucci & Brocato 1990

dependence on [α/Fe]

faint SN followed by C
Fe-fallaback

M
flat IMF
HN
followed by Zn

failed SN
O,Mg-fallback

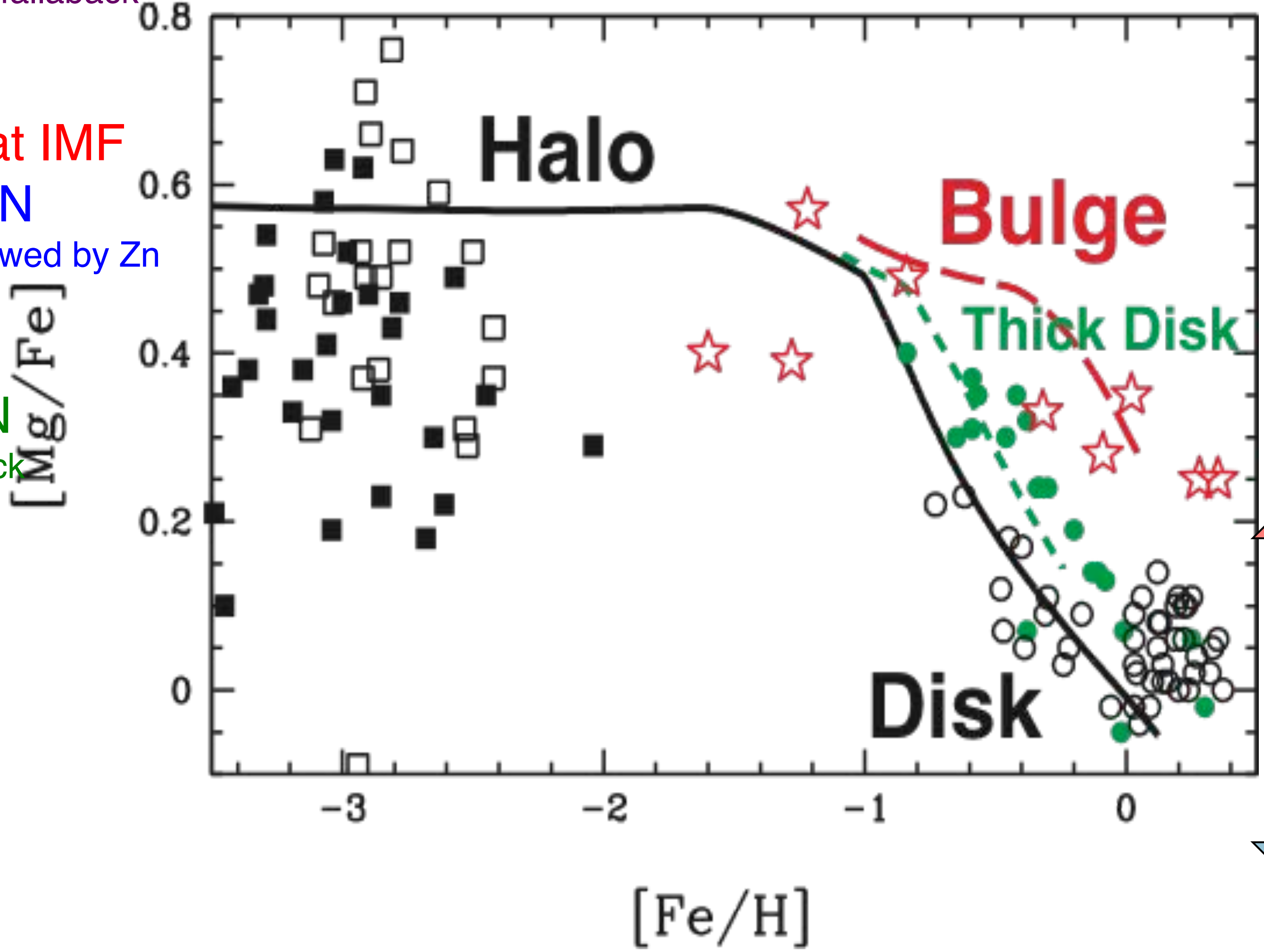

fast SF

SNIa
followed by Mn
slow SF

Nomoto et al. 2007 岩波

SFH of solar, thick disk, bulge, halo

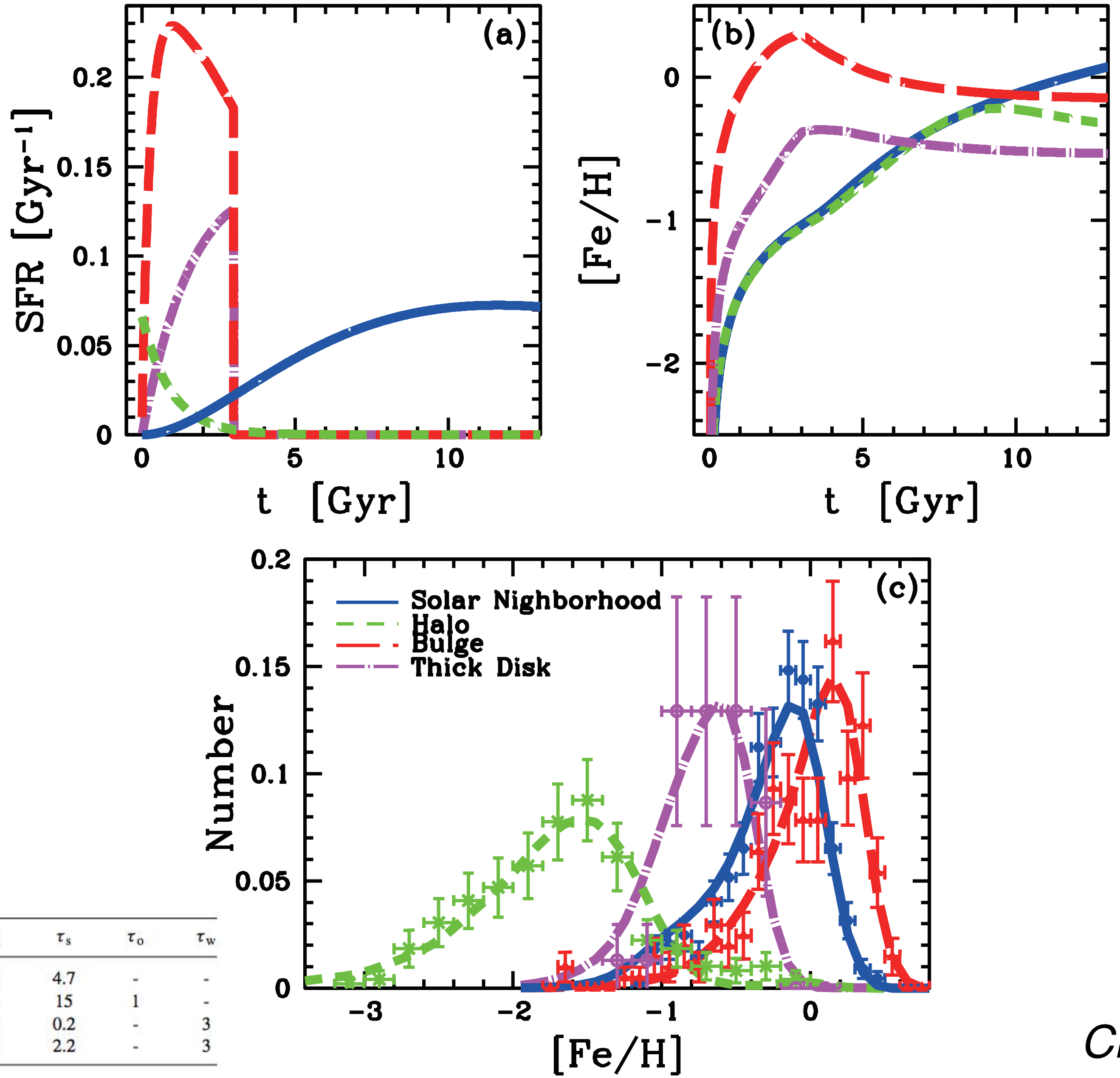

	τ_i	τ_s	τ_o	τ_w
Solar neighbourhood	5	4.7	-	-
Halo	-	15	1	-
Bulge	5	0.2	-	3
Thick disc	5	2.2	-	3

CK et al. 2011

Environmental Dependence

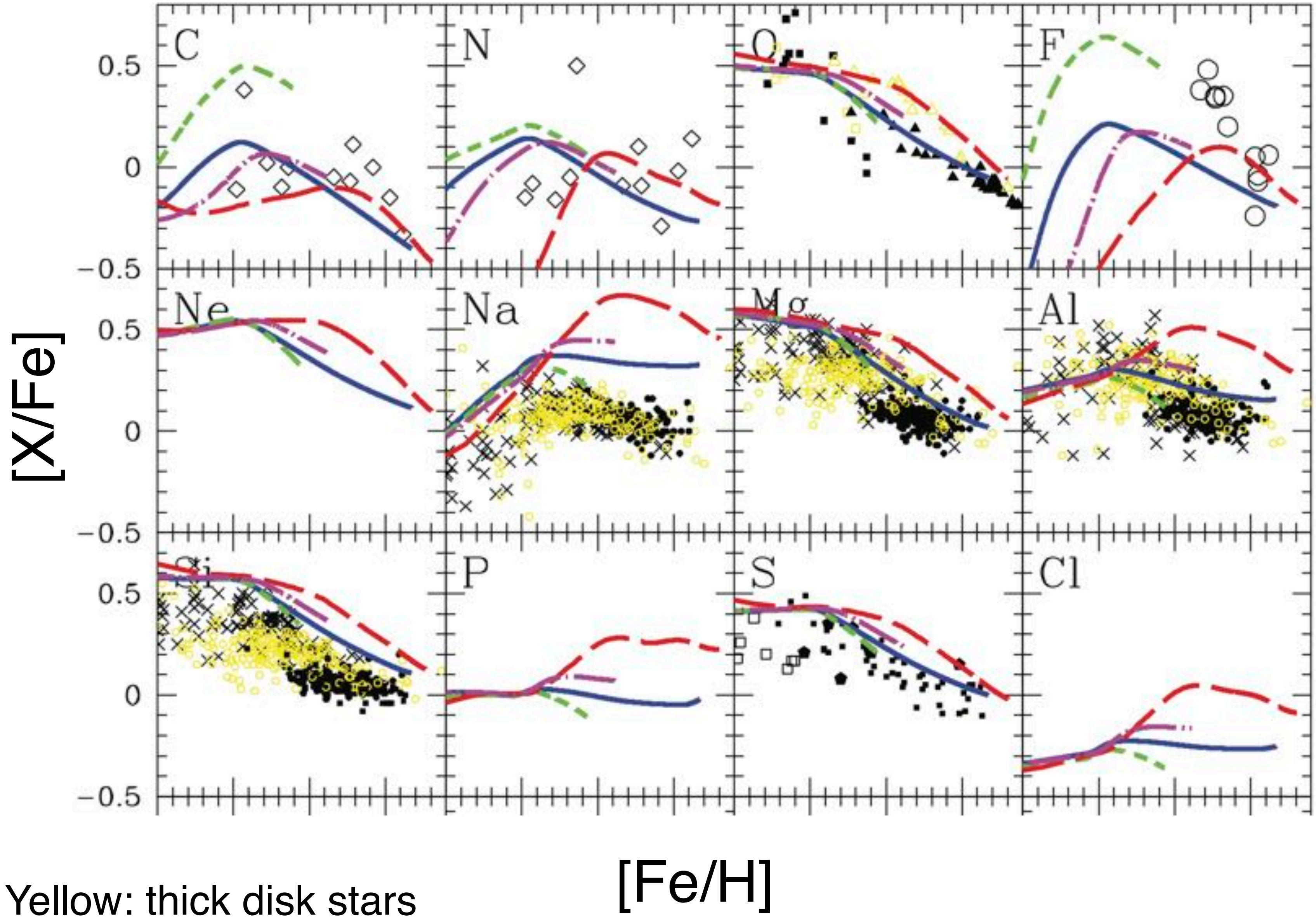

Yellow: thick disk stars

CK et al. 2011

Chemodynamical Simulations of a Milky Way-type galaxy

CK & Nakasato 2011

Scannapieco et al. 2012 (code comparison)

CK 2015

Chemodynamics

UV background radiation
(Haardt & Madau 1996)

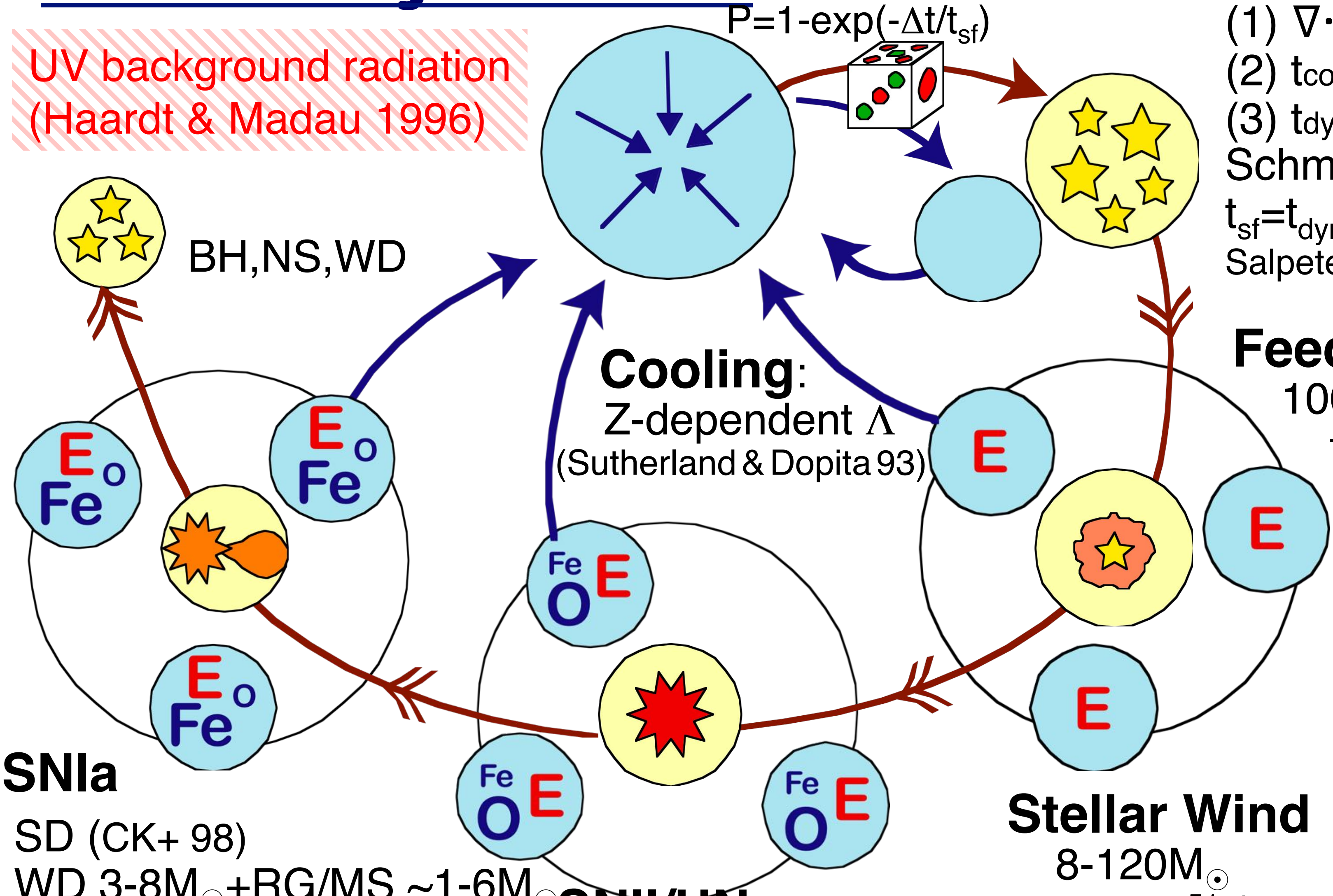

Star Formation
(1) $\nabla\cdot v<0$
(2) $t_{cool}<t_{dyn}$
(3) $t_{dyn}<t_{sound}$
Schmidt SFR
$t_{sf}=t_{dyn}/c$, c=0.1
Salpeter/Kroupa IMF

Feedback
100% thermal
to $N_{FB}\sim400$
or 1kpc

SNIa
SD (CK+ 98)
WD 3-8$M_\odot$+RG/MS ~1-6$M_\odot$
Z-effect: [Fe/H] > -1.1
1.3×10^{51} erg
W7 yields (Nomoto+ 97)

SNII/HN
8-50$M_\odot$/20-50$M_\odot$
$1\text{-}30\times10^{51\text{-}52}$ erg
M,Z,E dependent yields (CK+ 06)

Stellar Wind
8-120$M_\odot$
$0.2\times10^{51}\,(Z/Z_\odot)^{0.8}$ erg
1-6$M_\odot$ AGB yields

Milky Way-type galaxy

Initial Condition: λCDM fluctuated sphere with $\lambda \sim 0.1$, $r \sim 3$Mpc,
$M_{tot} \sim 10^{12}\ M_{\odot}$, $N_{tot} \sim 120.000$, $M_{gas} \sim 10^{6}\ M_{\odot}$, $M_{DM} \sim 10^{7}\ M_{\odot}$
(CK & Nakasato 2011, *ApJ, 729, 16*)

Face on

Edge on

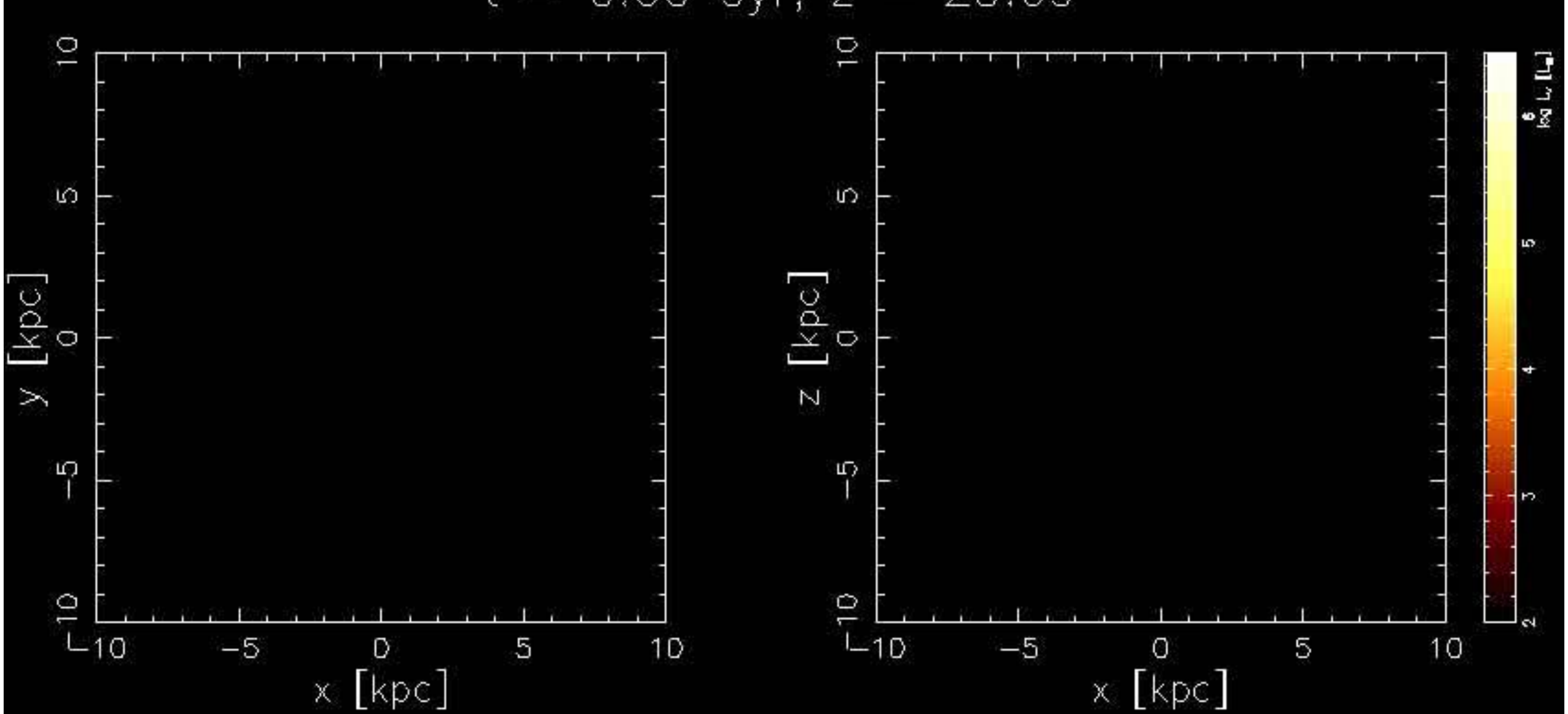

Similar results obtained also with Aquarius Initial Condition (CK 2015).

Star Formation History depends on environment

Bulge r<1, Solar Neighborhood: 7.5<r<8.5,|z|<0.5 kpc

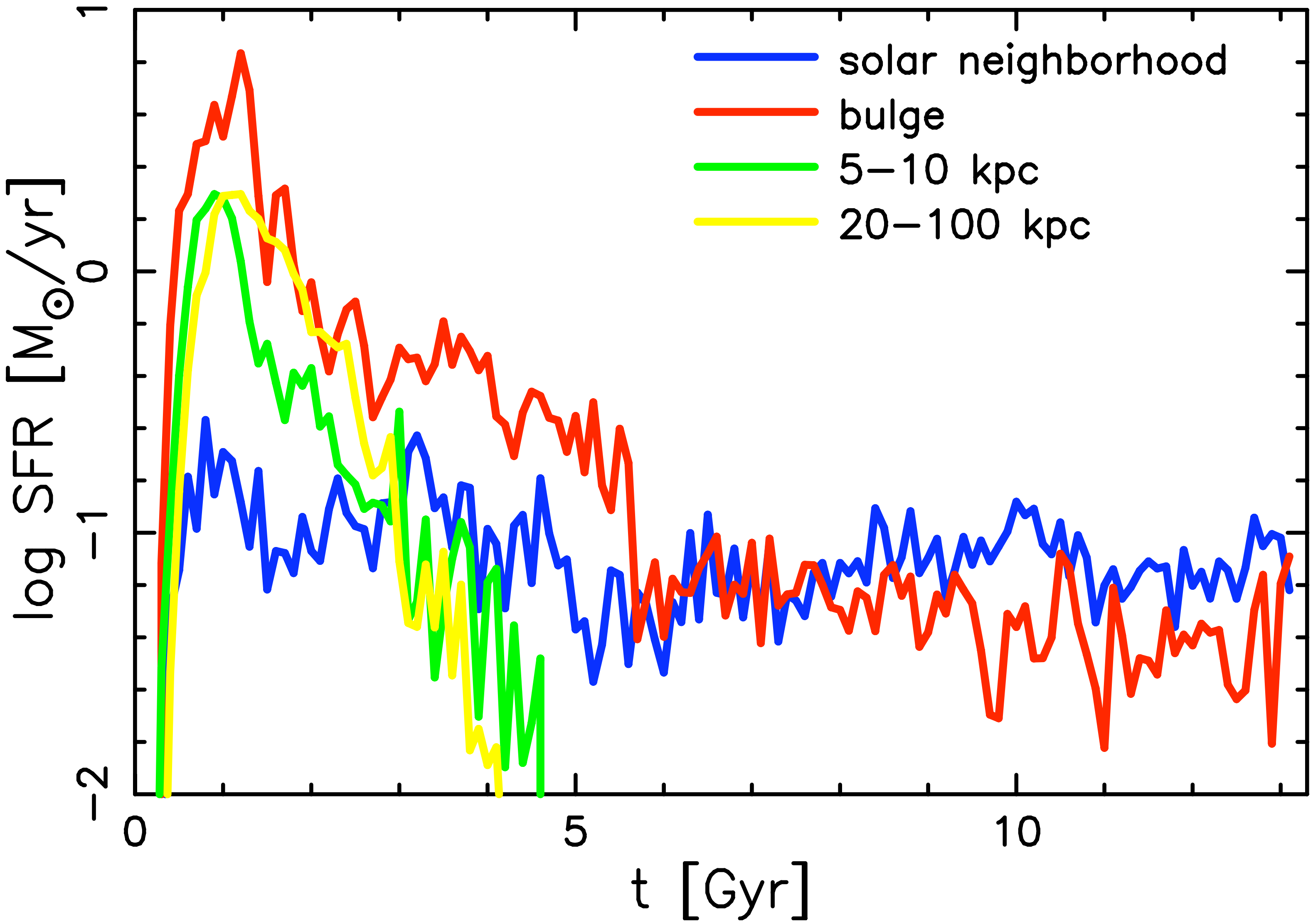

CK & Nakasato 2011

Metallicity Map

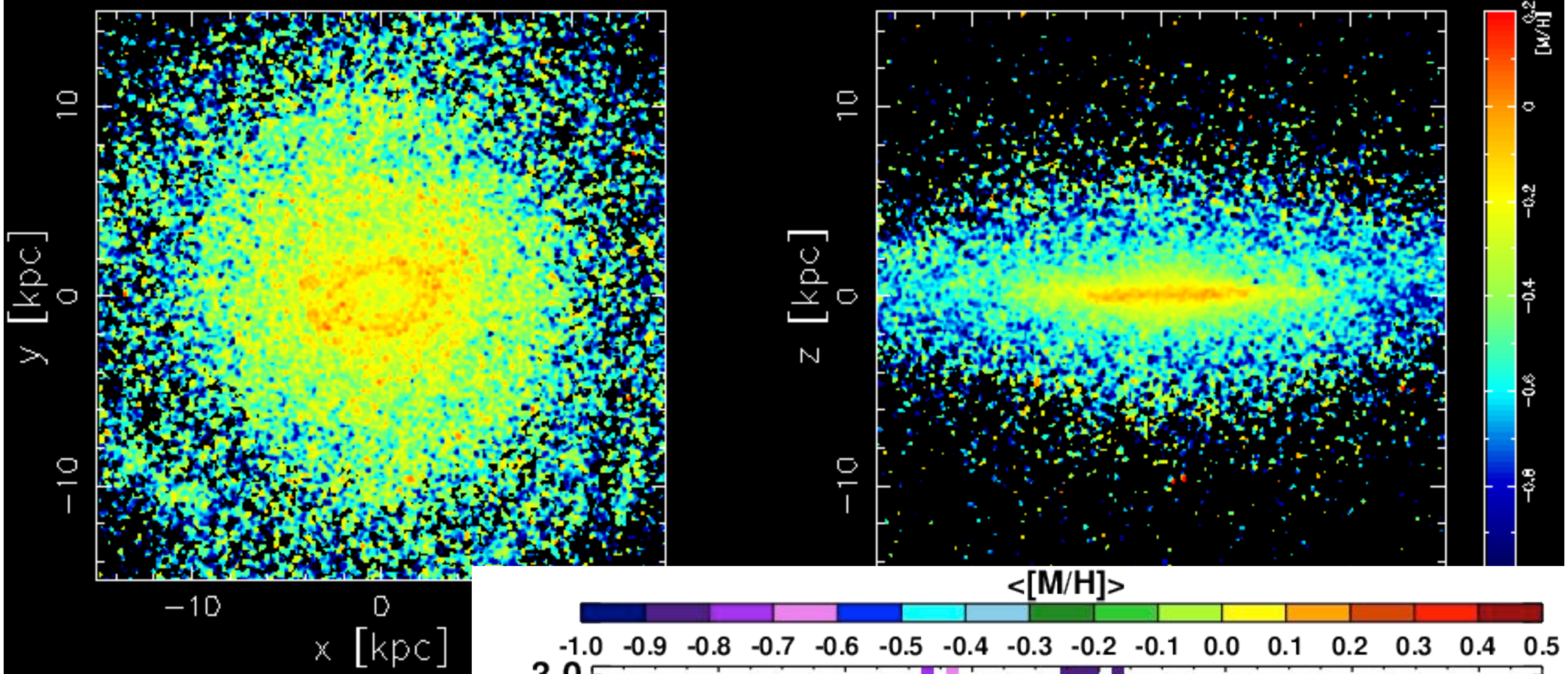

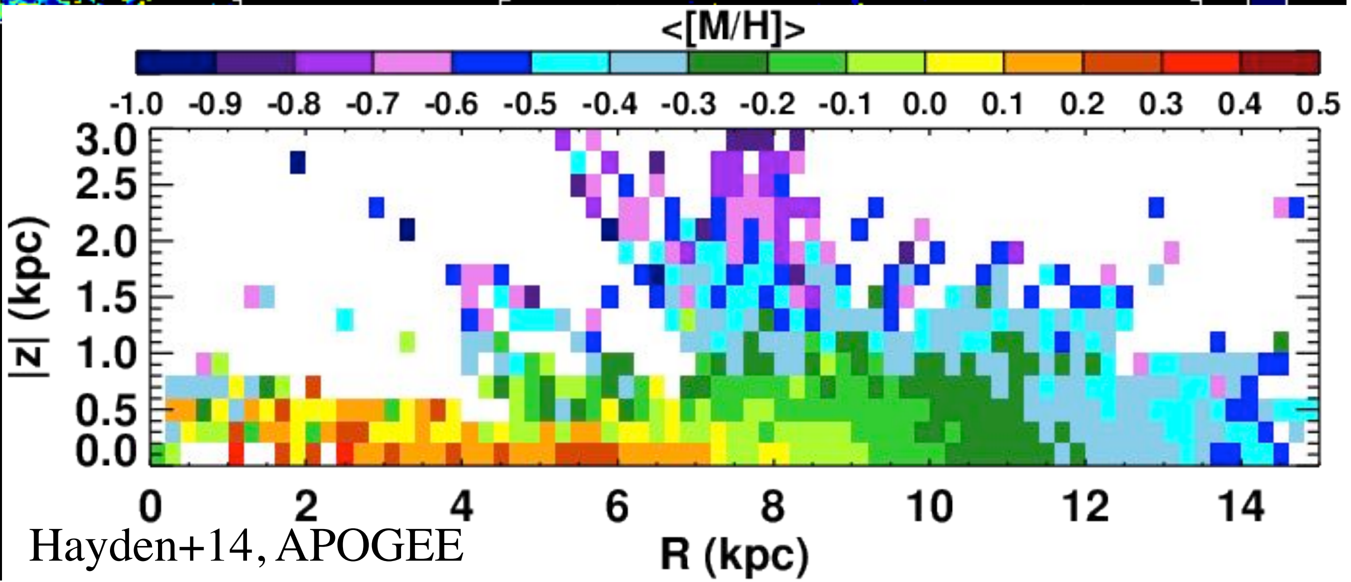

CK & Nakasato 2011

Hayden+14, APOGEE

Metallicity Gradients @ z=0

CK & Nakasato (2011)

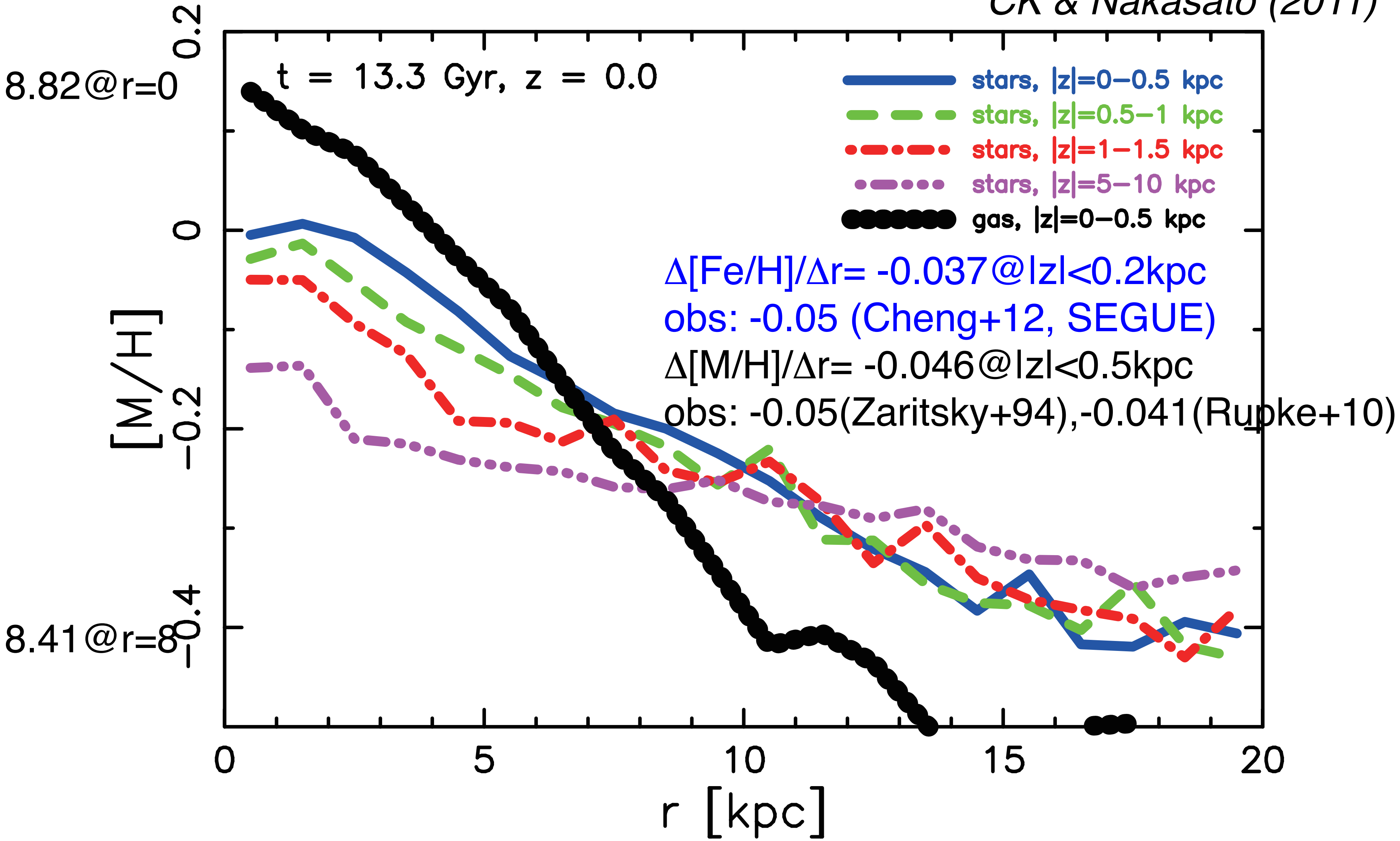

✶ Both radial and vertical gradients exist.

Evolution of Gradients

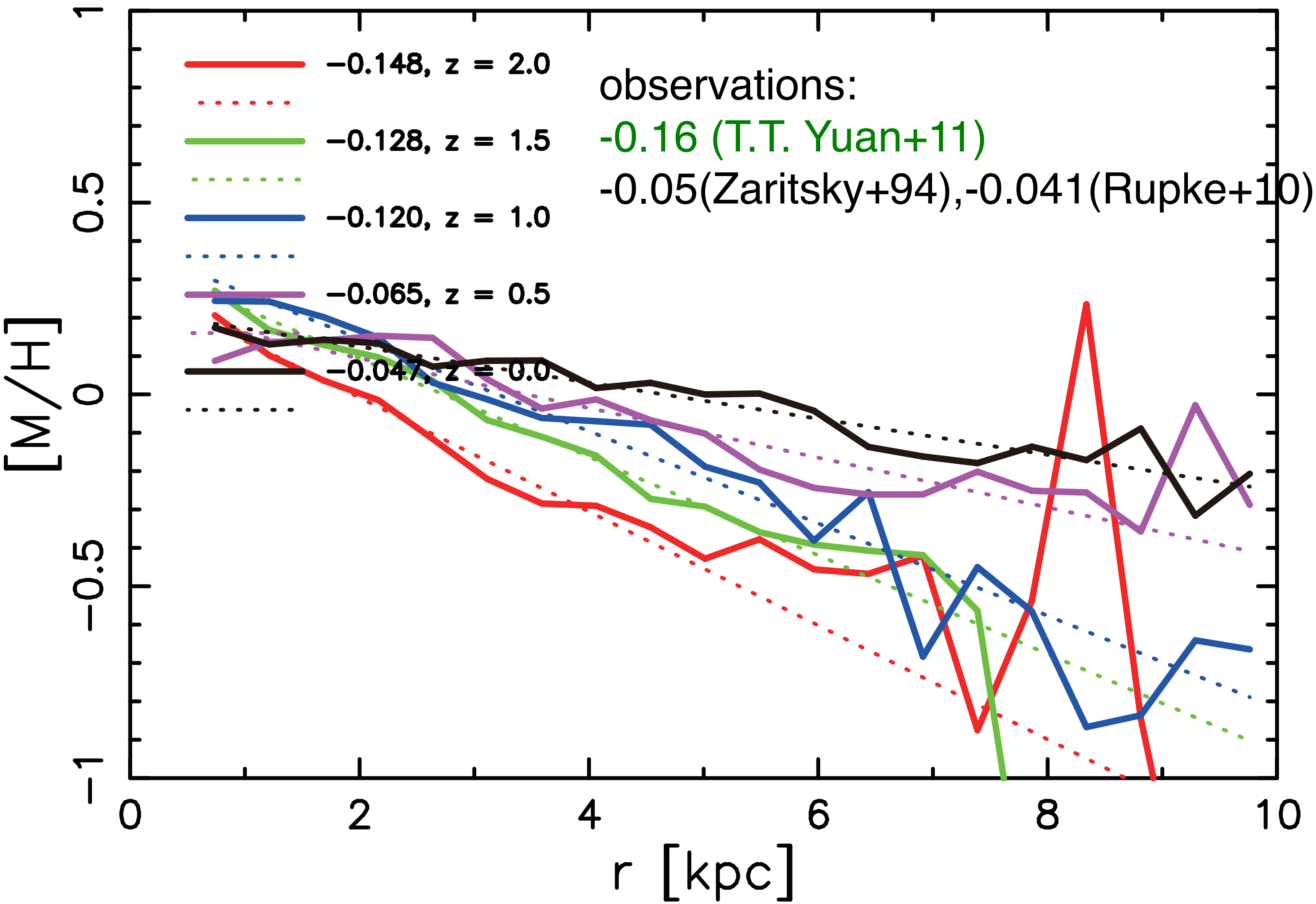

- Steeper (KN11), flatter (monolithic collapse), much steeper (migration) at higher-z. (also, Pilkington+12)

Age-Metallicity Relation

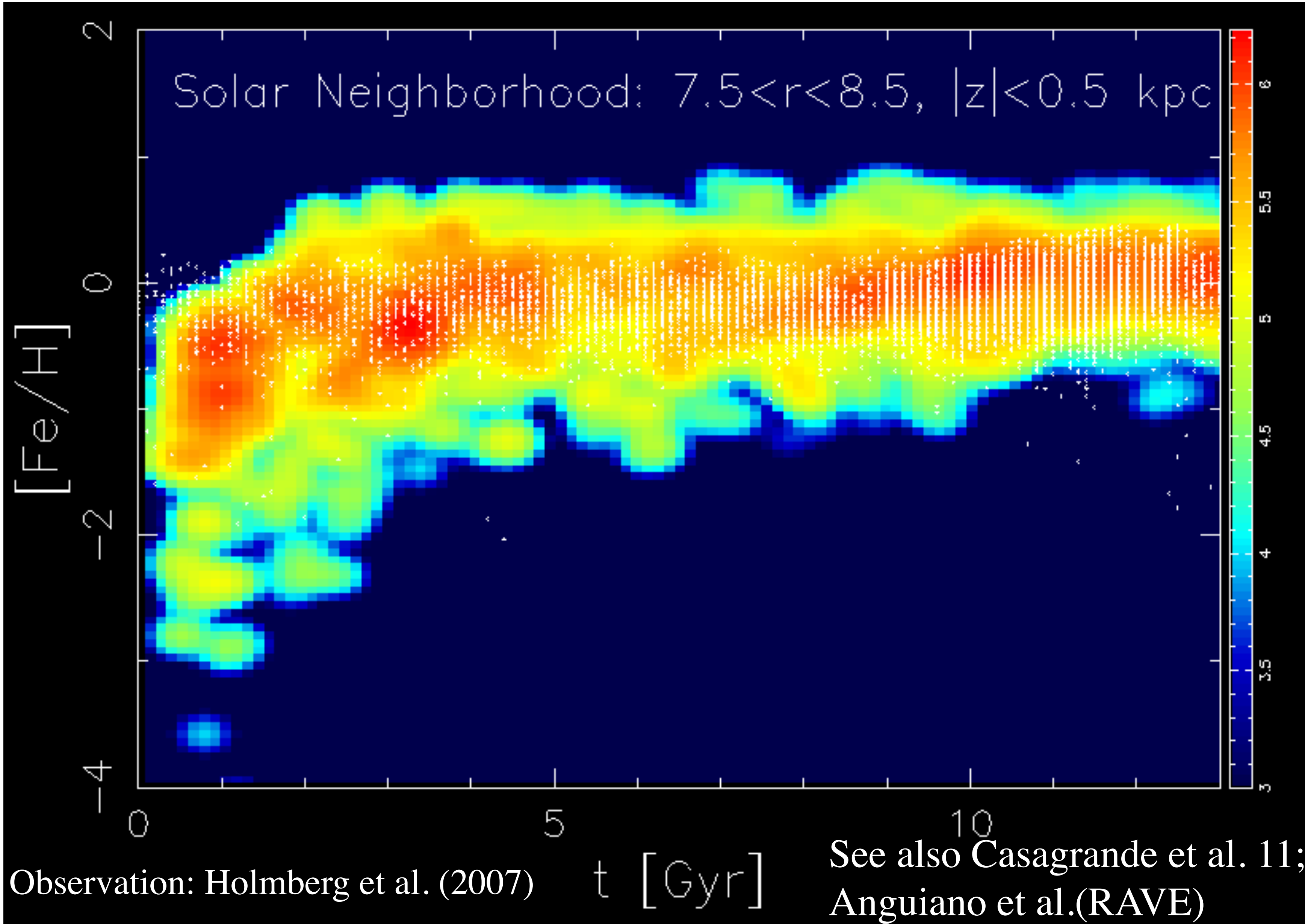

Observation: Holmberg et al. (2007)

See also Casagrande et al. 11;
Anguiano et al.(RAVE)

Age-Metallicity Relation

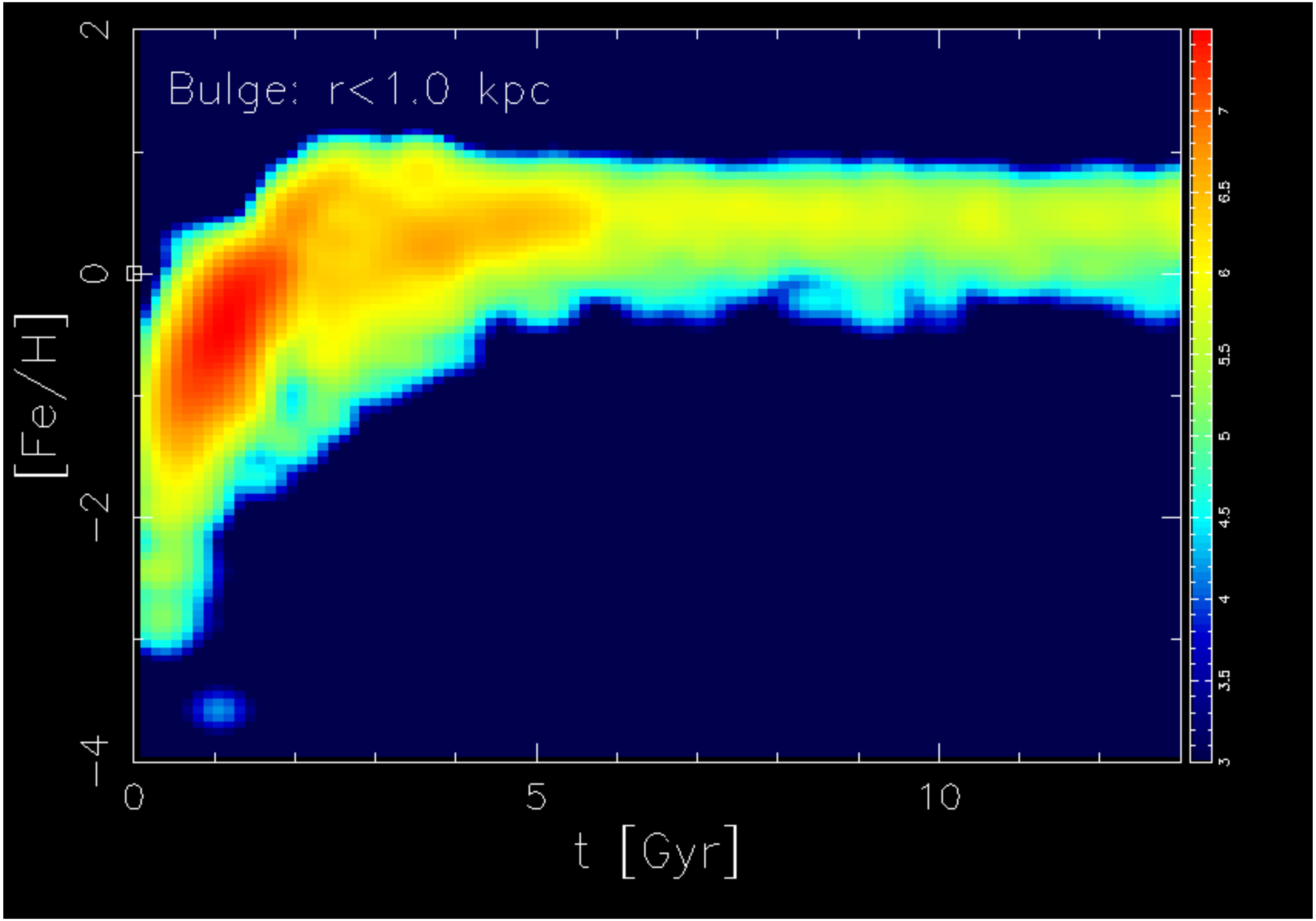

Age Metallicity Relation

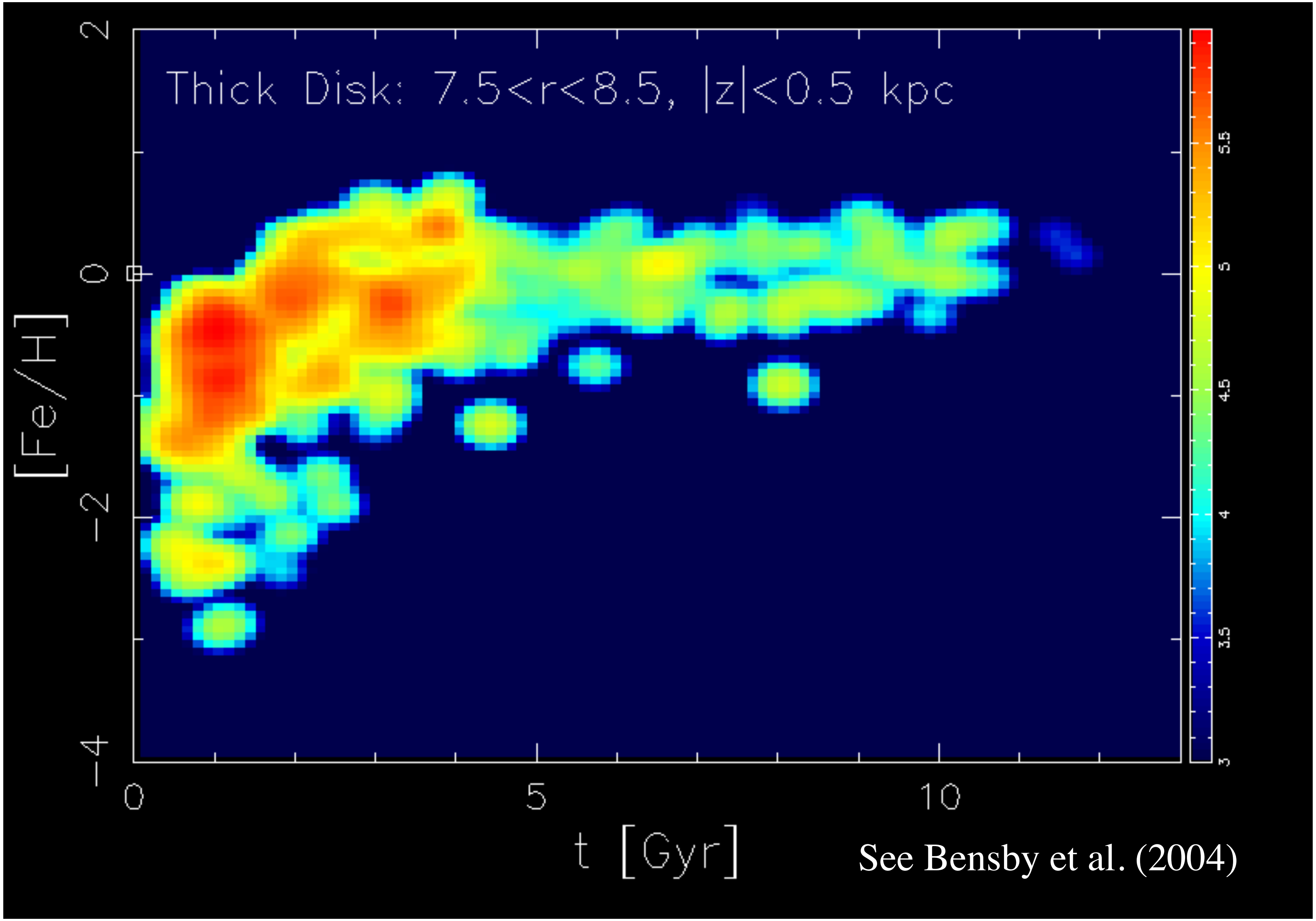

See Bensby et al. (2004)

Elemental Abundances (CK & Nakasato 2011)

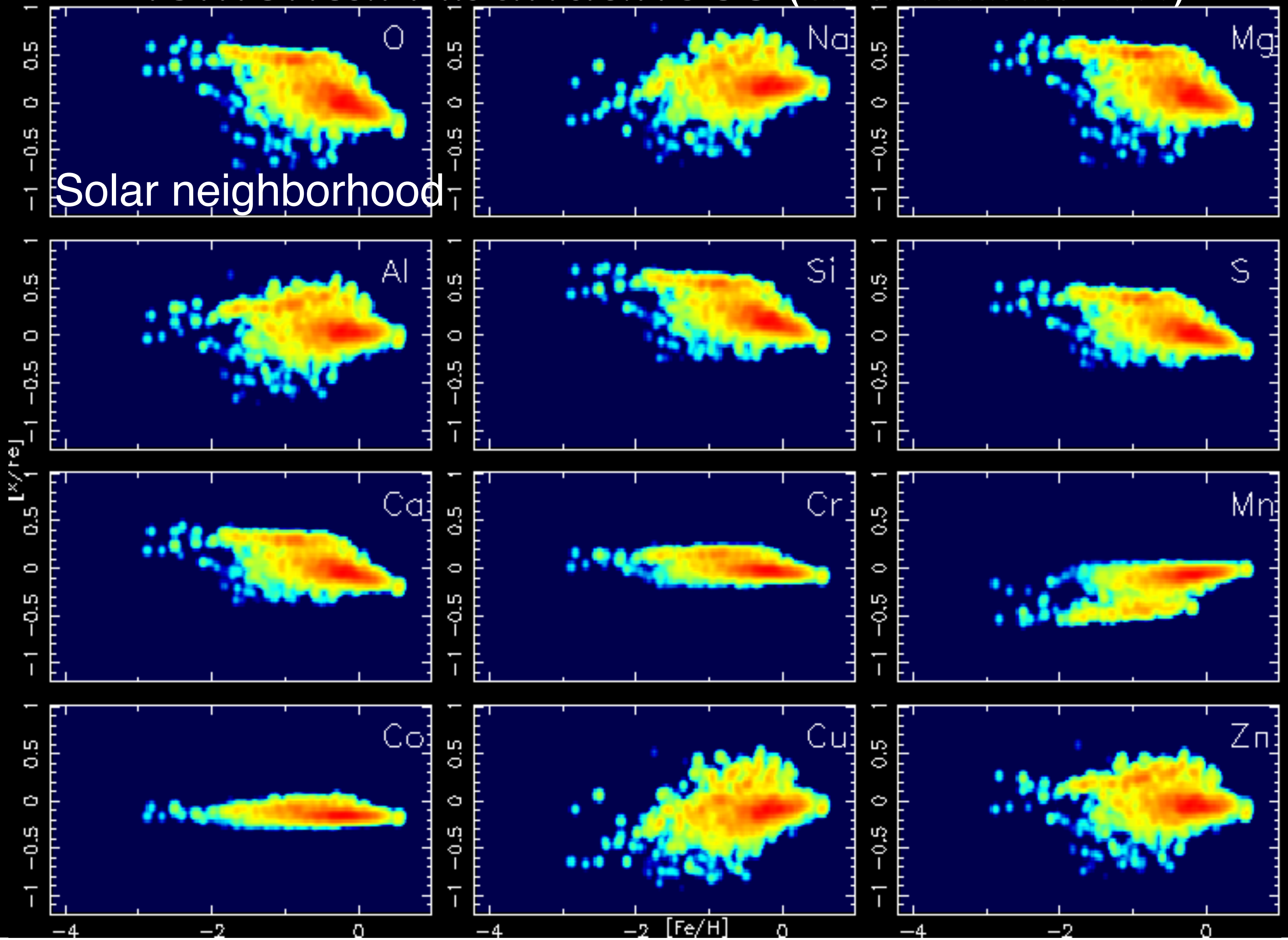

Elemental Abundances (CK & Nakasato 2011)

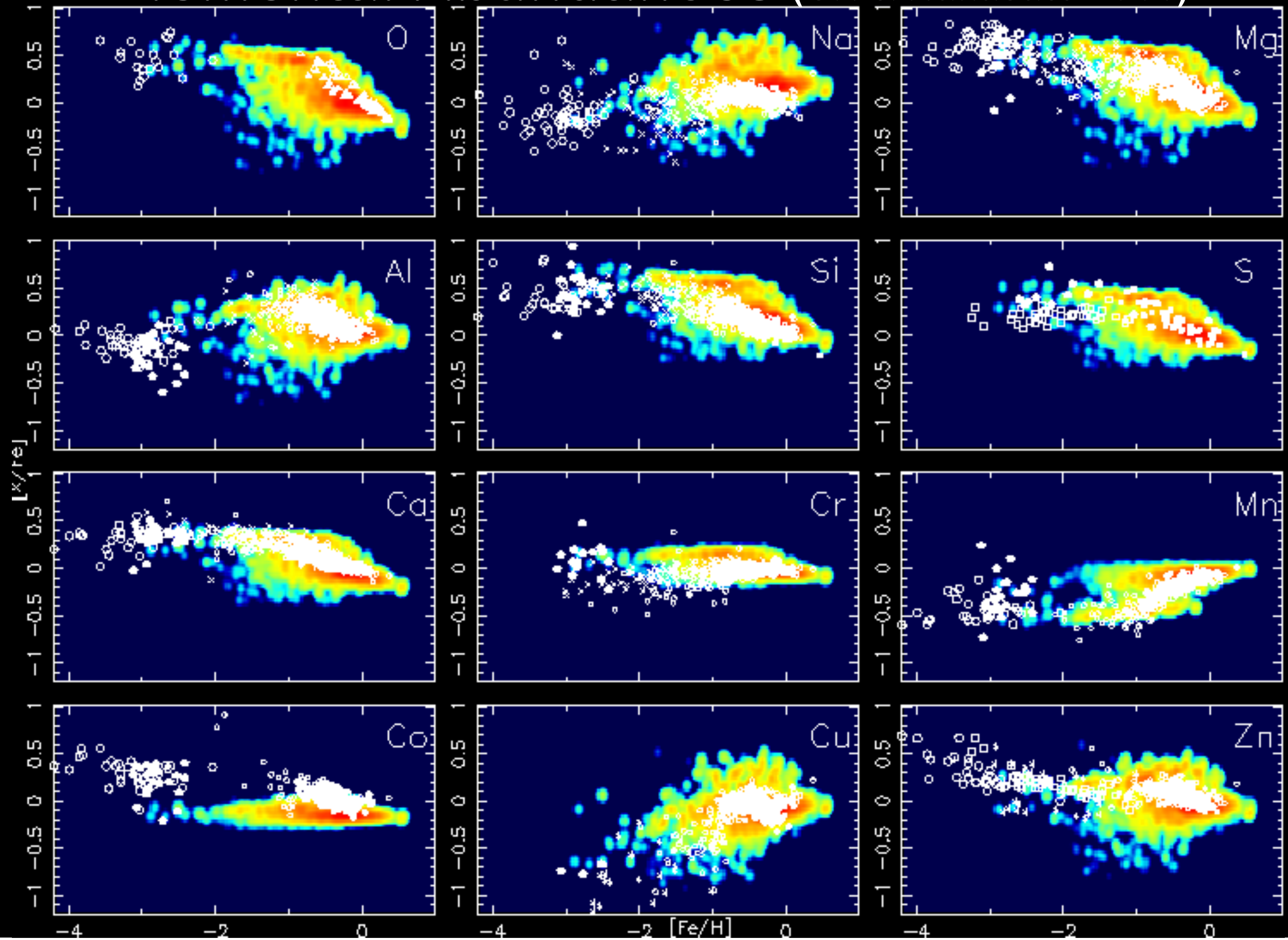

Elemental Abundances in Thick Disk

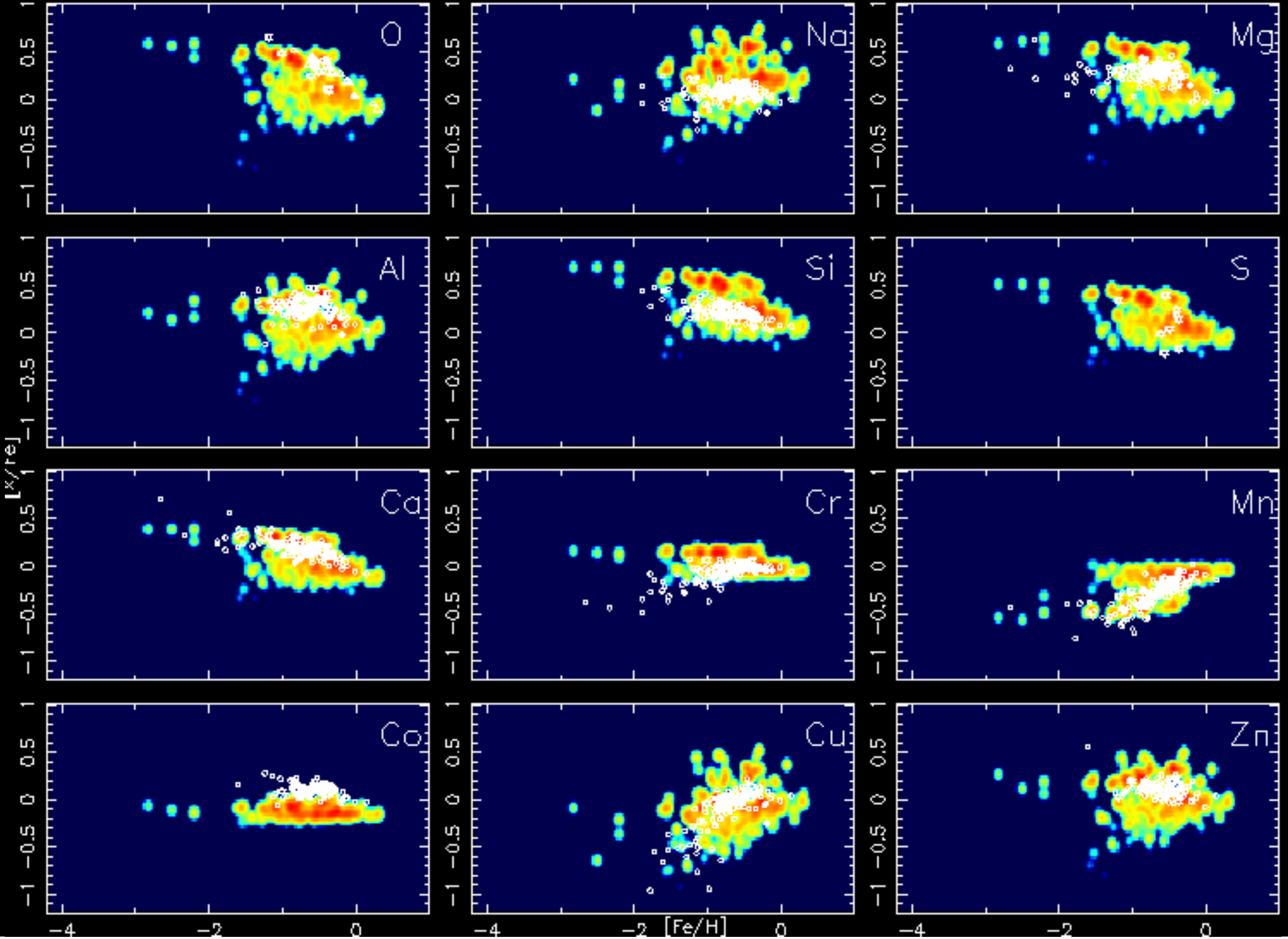

Elemental Abundances in Bulge

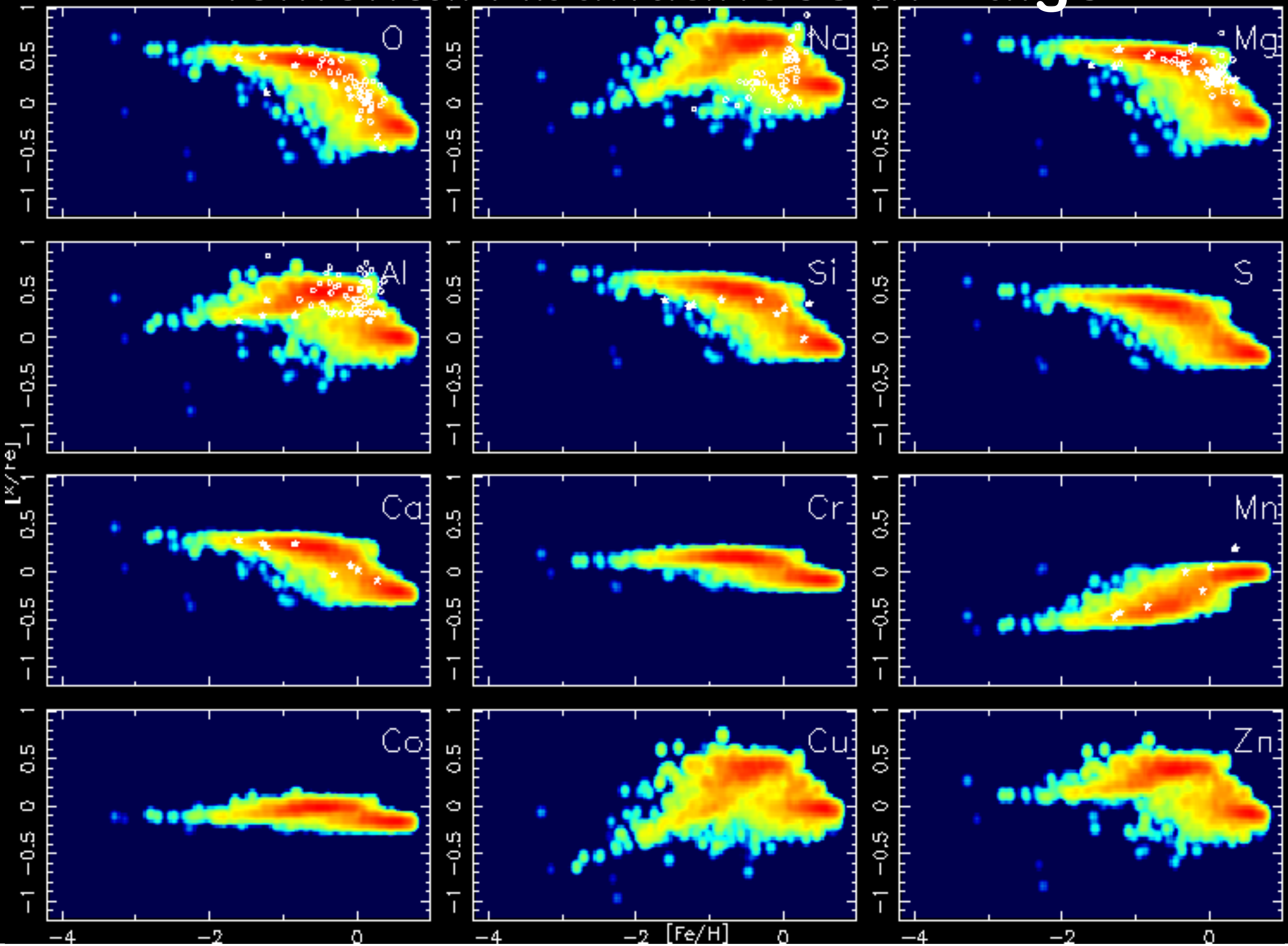

Inhomogeneous enrichment

The scatter of [X/Fe] at given [Fe/H] is increased/decreased by

1. Local variation in SF, inflow, outflow, and metal flows (**in-situ**
2. Mixing of stars due to dynamical effects (**accretion** of merging satellites, **migration,** disk heating/kick out).
3. Stellar yields depend on M,Z,E, rot. of stars (**intrinsic variation).**
4. ISM may be mixed before the next star formation by other effects e.g., diffusion and turbulence.

Therefore

- ★ No strong Age-Metallicity Relation.
- ★ Most metal-poor stars ≠ Oldest stars
- ★ Long-lifetime sources (e.g., AGB, NS mergers) can contribute at low metallicities

Galactic Archaeology

of Milky Way and local dwarf galaxies

- Motions of <u>one billion</u> stars are measured with GAIA.
- Elemental Abundances (from Li to Eu) of <u>million</u> stars will be measured with **multi-object spectrographs**:
  - **SEGUE** (Resolution~1800) on SDSS
  - **RAVE** (R~7500) on 1.2m UKST
  - **HERMES** on AAT (R~28000/50000)
  - **APOGEE** (R~20000, IR) on SDSS
  - **GAIA-ESO with VLT** (R~20000/40000)
  - ~~WFMOS on Subaru~~
  - **WEAVE** on WHT (R~5000/20000)
  - **4MOST** on VISTA (R~5000/18000)
  - **MSE/ngCFHT**
  - …

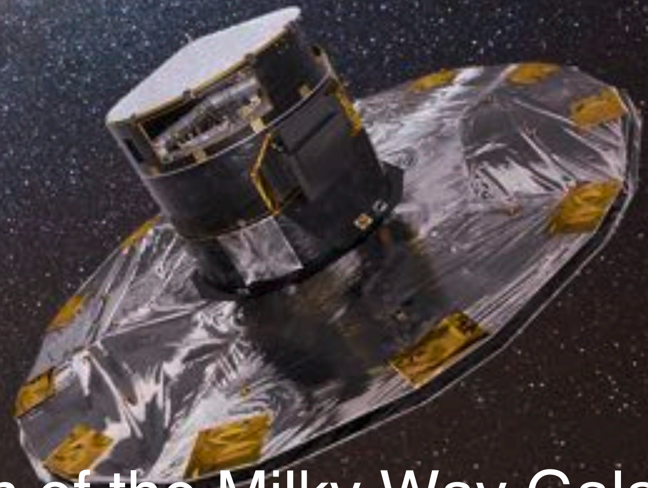

- Chemical and dynamical evolution of the Milky Way Galaxy will be revealed!

GAIA spacecraft http://sci.esa.int/gaia/